TÉCNICO LISBOA

Modeling of an aerated bioreactor under non ideal mixing conditions

Modeling improvement of enzyme production by *Trichoderma reesei*

Pedro Miguel Afonso Fernandes

Thesis to obtain the Master of Science Degree in

Chemical Engineering

Supervisor(s):
Dra. Prof. Helena Maria Pinheiro (IST)
Dr. Frédéric Augier (IFPEN)

Examination Committee

Chairperson: Prof.Francisco Manuel Lemos (IST)
Supervisors: Dr. Frédéric Augier (IFPEN)
Members of the Committee: Prof. Carla Rocha de Carvalho (IST)

December 2020

Declaration

I declare that this document is an original work of my own authorship and that it fulfills all the requirements of the Code of Conduct and Good Practices of the Universidade de Lisboa.

Acknowledgments

First I would like to thank my supervisors, Dr. Frederic Augier and Dr. Romain Rousset from IFPEN and Dra. Prof. Helena Pinheiro from IST for all their time, patience and availability to help me and explain me all the necessary subjects that allowed me to do this thesis with success.

To my family, specially my parents and grandmother, that always supported me and encouraged me to never give up and keep working hard to reach my goals in life.

To my friends (Tomás, Bruno, David, Guedes, Corte Real, Inês, Constança, Kika, Mariana, Jimenez, Ruben, Samouco, Dércio, Saltão, Gamelas and Lelé), who accompanied me in these last 5 years and were always there for me in the good and bad moments, helping me and motivating me whenever I needed it.

Finally, a very special thank to Maria Madalena Braga who has always been by my side for the past years helping me with everything I needed and always kept my spirits high when I was feeling less confident. A true companion that never gave up on me and always believed in me.

Abstract

The purpose of this thesis was to improve an existing kinetic model to enable it to predict the behaviour of *Trichoderma reesei* cultures producing cellulases in non-ideal mixing conditions in order to assist with scale-up problems. The modelling calculations were implemented in Virtual Basic language from Excel and the model was validated against experimental results obtained in the laboratory with single reactor and two reactor, aerobic-anaerobic, interconnected arrangements within the scope of a PhD thesis.

The model was improved by adapting its kinetics assumptions and including new features like the storage of lipids by the cells, the aging of the culture, the storage of oxidative power inside the cells and the presence of air bubbles in recirculation streams. The improved model was able to predict the behaviour of the laboratory cultures and provided new ideas to guide further investigations into the metabolism of cellulase production in *Trichoderma reesei* cultures.

The perfect mixing assumption was found to introduce only small deviations in the modelling results, in the laboratory experimental conditions.

Keywords: *Trichoderma reesei*, mechanistic modelling, cellulase production, Scale-up, non-ideal mixing conditions

Resumo

O objetivo desta tese foi o melhoramento de um modelo cinético existente para possibilitar a previsão do comportamento de culturas de *Trichoderma reesei* ao produzir celulases em condições não-ideais de mistura, de modo a estudar problemas de *scale-up*. As equações do modelo foram implementadas em linguagem *Virtual Basic* do Excel e o modelo foi validado com resultados experimentais obtidos no laboratório com um reator e dois reatores, aeróbio-anaeróbio,interconectados, dentro do âmbito de uma tese de doutoramento.

O modelo foi melhorado adaptando a cinética do microorganismo e incluíndo novas características no modelo, como o armazenamento de lípidos pelas células, envelhecimento da cultura, armazenamento de poder oxidativo pelas células e presença de bolhas de ar nas correntes de recirculação. O modelo melhorado foi capaz de prever o comportamento das culturas laboratoriais e forneceu novas ideias para guiar futuras investigações sobre o metabolismo de produção de celulases em culturas de *Trichoderma reesei*.

A suposição de mistura perfeita introduziu apenas pequenos desvios nos resultados modelados, nas condições experimentais laboratoriais.

Keywords: *Trichoderma reesei*, modelação mecanistica, produção de celulase, *Scale-up*, condições não-ideais de mistura

Contents

List of Tables

List of Figures

Acronyms

BTX Benzene-toluene-xylene.

CBM Carbohydrate-binding module.

CD Catalytic domain.

CFD Computational fluid dynamics.

DO Dissolved oxygen.

DP Degree of polymerization.

FAME Fatty acid methyl ester.

IFPEN *Institut Français du Pétrole - Energies nouvelles*.

OTR Oxygen transfer rate.

RTD Residence time distribution.

SmF Submerged fermentation.

SSF Solid state fermentation.

UNFCC United Nations Framework Convention on Climate Change.

Chapter 1

Introduction

The world energy demands have been satisfied by the use of fossil fuels and as a consequence the greenhouse gas emissions have been increasing, resulting in several climate changes issues (Dahman et al. 2019). The rising of fossil fuels prices and the international pressure on climate change mitigation have increased the need to develop renewable sources of energy (Dahman et al. 2019). Pressing concerns related to climate have led the world to use other sources of fuels like biofuels that are produced from biomass (Dahman et al. 2019). The United Nations Framework Convention on Climate Change (UNFCC) stated that biomass is a nonfossilized and biodegradable organic substance.

Biofuels production has been increasing for the past years reaching a record of 154 billion litres in 2018 (International Energy Agency). The U.S. Department of Agriculture and U.S. Department of Energy determined that 20% of the transportation energy and 25% of chemicals will be produced from biomass by 2030 (Fan et al. 2017). One of these biofuels is bioethanol produced from lignocellulosic biomass. The major component of this biomass is cellulose, a polymer of glucose molecules. The monomers of glucose are obtained by enzymatic hydrolysis of the biomass cellulose to then be used in a fermentation process to produce ethanol. The production of enzymes for the hydrolysis of cellulose is a key step of this production process and IFPEN teams have been optimizing a process for this purpose.

This process consists on the employment of cultures of *Trichoderma reesei*, a filamentous fungus with a great capacity for secretion of hydrolytic enzymes. In order for the process to be economically feasible it is required the use of big bioreactors with hundreds of cubic meters' capacity. For that it is mandatory to do the scale-up of the process which implies studying its impact on the culture performance due to the condition changes from the lab scale to the industrial scale. Currently a PhD student at IFPEN, Tamiris Roque Gonçalves, is using a scale down methodology to study the impact of fermentation broth heterogeneities, induced by the scale-up, on the production of enzymes.

The aim of the present thesis is to improve an existing bioreactor model in order to adapt it to heterogeneous conditions by adding new bio-kinetic mechanisms. To validate the model, the experimental results from the PhD work already mentioned, were used. This thesis is composed of two parts. The first is related with single reactor cultures that were performed in the laboratory with different production conditions and the objective is to identify a relation between the model parameters and the results from the different conditions that were used in each culture. The second part constitutes the main scope of this thesis that is the modelling of the behaviour of cultures in non ideal mixing conditions to understand the impact on the production during the scale-up of the process.

Chapter 2

State of the Art

2.1 Biofuels

Biofuel are produced from biomass feedstocks such as plants or organic waste. The most known are bioethanol and biodiesel. These type sof fuels, can help reduce the emissions of CO_2 and the dependency of the world on crude oil, as a primary source of energy, mitigating the global warming problem because the amount of carbon dioxide that is released by the combustion of the biomass, is the same that is absorbed by the plants during photosynthesis. This means that the CO_2 concentration in the atmosphere remains the same (Gavrilescu 2014). There are two main types of biofuels, depending on its feedstock: the first generation and the second generation. Moreover, another has recently gained attention by the scientific community: the third generation of biofuels (Alam et al. 2015)

2.2 First Generation Biofuels

First generation biofuels are produced from food crops (edible biomass) such as sugar cane, corn, soybean, vegetable oils and starch extracted from cereals. Not all parts of these plants are useful for the food processes, just the edible part, but still their use creates competition between the biofuels and the food market (Herve et al. 2011; Naik et al. 2010). A major consequence of this competition is the rise of food prices that affects World economics (Laursen W. 2006; Hossain et al. 2019).

One of the most characteristic examples of this type of energy sources is biodiesel that is produced from the transesterification of vegetable oils. This process consists on a chemical reaction between these oils and methanol that results in FAME (Fatty Acid Methyl Ester) with properties that are close to those of diesel. Another first generation biofuel that is very popular, especially in Brazil and in the USA, is the bioethanol from sugar cane and corn (Bertrand et al. 2011). Both crops are used as a source of sugars that can be then fermented by yeasts or bacteria to produce bioethanol (Bertrand et al. 2011).

Unfortunately there have been concerns about the impact on biodiversity and land use which imposed the need to limit the production of this type of fuels (Naik et al. 2010; Herve et al. 2011). In response to these problems another type of biofuels emerged and has obtained a lot of attention lately which is the second generation of biofuels.

2.3 Second Generation Biofuels

Contrary to the first generation of biofuels the second generation does not compete with the food market for resources since it uses non-food crops and their wastes, agricultural residue and wood chips,

as sources of lingocellulosic biomass feedstock (Dahman et al. 2019).

Besides being a non-food resource, lignocellulose has also the advantage of being cheaper than the biomass used for the first generation of biofuels (Naik et al. 2010). Moreover, the second generation of biofuels allows an average reduction of greenhouse gases emissions of 70% when compared with the values from fossil fuels, while first generation biofuels only reduce these emissions by 30% (Jourdier 2012).

There are two main routes to transform the lignocellulose materials into fuels: the thermochemical and the biochemical. The first consists on a gasification of the biomass to produce syngas, a mixture of H_2 and CO, that can then be fed to a Fischer-Tropsch process to obtain diesel and kerosene. The second starts with the hydrolysis of biomass into sugars which are then fermented to produce bioethanol that can be blended with gasoline in volume ratios from 5% to 25% (Shelley Minteer 2016).

The lignocellulosic ethanol has been studied a lot in the past decades and has gained much attention as a promising renewable source of transport fuel (Sigoillot and Faulds 2011). However, since then there have been problems with the development of an economical process for its large scale production, due to several technical barriers (Naik et al. 2010). So, there is the need to strengthen financial structures to promote the set off of second generation biofuels, in particular the commercialization of cellulosic ethanol (Global Agriculture Information Network 2015).

2.4 Second Generation Bioethanol

Like mentioned before the bioethanol from second generation is produced using lignocellulosic biomass that is obtained from agriculture waste, forestry residues, urban and industrial waste among other, not compromising the food security (Nigam and Singh 2011).

Among the liquid biofuels that are known, bioethanol possesses a great potential as a substitute to conventional gasoline thus replacing the fossil fuels that are responsible for the release of big amounts of greenhouse gases to the atmosphere (Dias et al. 2013). Also, bioethanol can improve significantly some fuel properties of gasoline, like the octane number and the efficiency of combustion, when blended with it (Pejin et al. 2009). It allows also a cleaner combustion process, reducing the amount of CO produced as well as unburned hydrocarbons and NO_x in the exhaust gases (KÜÜT et al. 2011).

Due to the complexity of the structure of lignocellulose the production of ethanol from it requires certain steps (Arora et al. 2019):

1. Physical-chemical pre-treatment of the lignocellulosic materials to free the cellulose from the recalcitrant matrix;
2. Saccharification or hydrolysis of the cellulose to fermentable sugars;
3. Fermentation to convert sugars into ethanol;
4. Distillation to separate and purify the ethanol from the broth.

The hydrolysis step can be performed following an enzymatic route or a chemical one, for example with acid solutions (Cardona et al. 2010). However, the enzymatic hydrolysis is more promising than the acidic one, since the yield on glucose is higher (Cardona et al. 2010), the utility costs are lower (Sun and Cheng 2002) and it is more environmentally friendly (L. Rocha-Meneses et al. 2017). Saccharification represents 20% of the total costs of the lignocellulosic bioethanol production and it is affected by various parameters like the pre-treatment conditions, substrates concentration and enzyme activity (Sun and Cheng 2002).

To reduce the costs associated with the enzymatic hydrolysis, engineers have started to consider onsite production of enzymes (Simo Ellilä et al. 2017). This means that enzyme production can be done simultaneously with the hydrolysis of cellulose in the same reactor in an attempt to reduce the costs of enzyme recovery. However with the progression of the process the glucose obtained from the hydrolysis will build up causing it to inhibit enzyme production at a certain point (Chen 2014). So a separate production of hydrolytic enzymes has been considered and investigated. This way another step is added to the process, taking place as a part of Saccharification.

2.5 Lignocellulosic Biomass

Lignocellulose, is a biological resource composed by three main macromolecules that are connected between them by covalent bonds: cellulose (40-60%), hemicellulose (20-40%) and lignin (10-25%) (McKendry 2002). The content of each component depends on the type of biomass material, its variety, growth conditions and maturity (Tye et al. 2016).

Cellulose is the main component of cell walls and the most abundant biological resource on earth (Jarvis 2003). It is a linear polymer of D-glucose linked by β-1,4-glycosidic bonds. The hydrogen links between the cellulose molecules gives it a rigid, fibrous and crystalline structure that confers it chemical stability and mechanical strength making it insoluble in water and resistant to degradation. Typically, cellulose molecules interact with hemicellulose forming complexes between the two molecular structures. These structures inhibit the access of enzymes which affect hydrolysis rates, and consequently the digestion of the lignocellulose and the production of fermentable sugars. Raud et al. (2014) showed that the greater the cellulose content in the biomass material the greater the yield in glucose and ethanol.

Hemicellulose, ranked second in abundance in the lignocellulosic biomass , has different sugars in its constitution like, D-glucose, D-galactose, D-mannose, D-xylose, L-arabinose and also uronic acids (Robak and Balcerek 2018). In contrast to the linear cellulose molecules, hemicellulose has a high degree of branching, giving it an amorphous structure that makes it less compact. Hemicellulose also has a lower degree of polymerization in comparison with cellulose (Patel and Parsania 2018). The degree of polymerization (DP) consists on the number of units present in a polymer (Arora et al. 2019) and the cellulose has a DP 10 -100 times bigger than hemicellulose (Patel and Parsania 2018). These properties of hemicellulose makes it more easily hydrolysed than cellulose (Jacobsen and Wyman 2000). The molecules of this polymer act as a supportive matrix for the cellulose microfibrils, wrapping around them, which means that it is necessary to remove it to increase the cellulose degradability (L. Rocha-Meneses et al. 2017). According to Zabed et al. (2016) an increase in hemicellulose ablation, increases the access to the cellulose polymers and consequently its hydrolysis rate.

Lignin is a complex aromatic heteropolymer composed by *p*-hydroxyphenyl , guaiacyl, and syringyl monomers (L. Rocha-Meneses et al. 2017). As a non-sugar based polymer, it cannot be used as a source of fermentable sugars, contrary to cellulose and hemicellulose. Its recalcitrant characteristics make it a physical obstacle to the hydrolytic action of enzymes (Percival Zhang et al. 2006). Furthermore, this undesirable component connects all the constituents of lignocellulose together which makes it further insoluble in water and more difficult to digest (L. Rocha-Meneses et al. 2017). Thus the greater the amount of lignin in the biomass materials the more difficult will be the hydrolysis of the cellulose and hemicellulose compounds. It is mandatory to remove the lignin from the lignocellulosic feedstocks so that enzymes can have easier access to the sugar based polymers in order to promote the saccharification.

Even though lignin cannot be utilized as a source of substrates for biological ethanol production, engineers found others ways to use it in the bioethanol production process in order for it to become

more profitable (Nigam and Singh 2011). Lignin compounds can be recovered from the pre-treatment of the lignocellulosic biomass and fed to thermochemical processes to produce heat and electricity to the biorefinery plants as well as syngas and bio-oil to produce fuels (Nguyen et al. 2019). Besides this energetic pathway the lignin, as a unique aromatic polymer, can also serve as a feedstock to produce several chemical products like phenols, benzene-toluene-xylene (BTX), bioplastics, resins, adhesives, dimethyl ether and many others (Nguyen et al. 2019; Cherubini and Strømman 2011). So the lignin starts to be seen as a by-product of the lignocellulosic ethanol process (Fan et al. 2017), instead of a waste.

2.6 Cellulases

The hydrolysis of lignocellulosic biomass requires the intervention of several enzymes at the same time with different activities, that act in synergy (Abu-Ghannam and Balboa 2018).

The hydrolytic enzymes that are used to digest the cellulose molecules into glucose are normally called cellulases.

The cellulase enzymes are constituted by modules which determine their way of action (Jayasekara and Ratnayake 2019). There are catalytic modules and non-catalytic modules (Jayasekara and Ratnayake 2019). The non-catalitic carbohydrate-binding module (CBM) is connected to a catalytic domain (CD) through a linker (Soni et al. 2018). The CBM binds to the cellulose fibrils by adsorption and penetrates them and the catalytic domain starts to cut the chain as can be seen in Figure 2.1 (Soni et al. 2018).

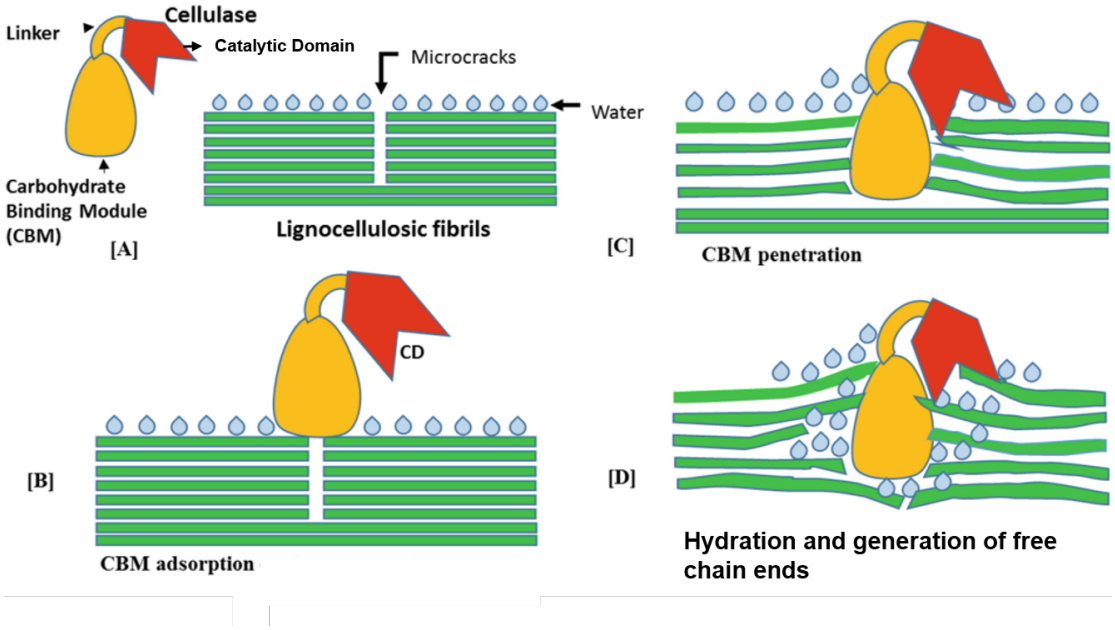

Figure 2.1: Schematic representation of the action of cellobiohydrolase I (Exoglucanase) in cellulosic fibers. Adapted source: (Soni et al. 2018).

The hydrolysis of cellulose requires the combined action of three different types of cellulases and each one has a specific role to play in the process (Jayasekara and Ratnayake 2019; Mojsov 2016):

1. Endoglucanases (1,4-β-d-glucanohydrolase, EC 3.2.1.4), randomly attacks the internal bonds creating new chain ends;

2. Exoglucanase (1,4-β-d-glucan cellobiohydrolase, EC 3.2.1.91), acts on the ends of the cellulose chains that were generated before by the endoglucanases, to produce cellobiose (chains composed by two glucose molecules);

3. β-Glucosidase (β-d-glucoside glucohydrolase, EC 3.2.1.21) is finally responsible for the hydrolysis of cellobiose molecules into glucose.

In Figure 2.2 the different roles of cellulases in the cellulose hydrolysis are presented.

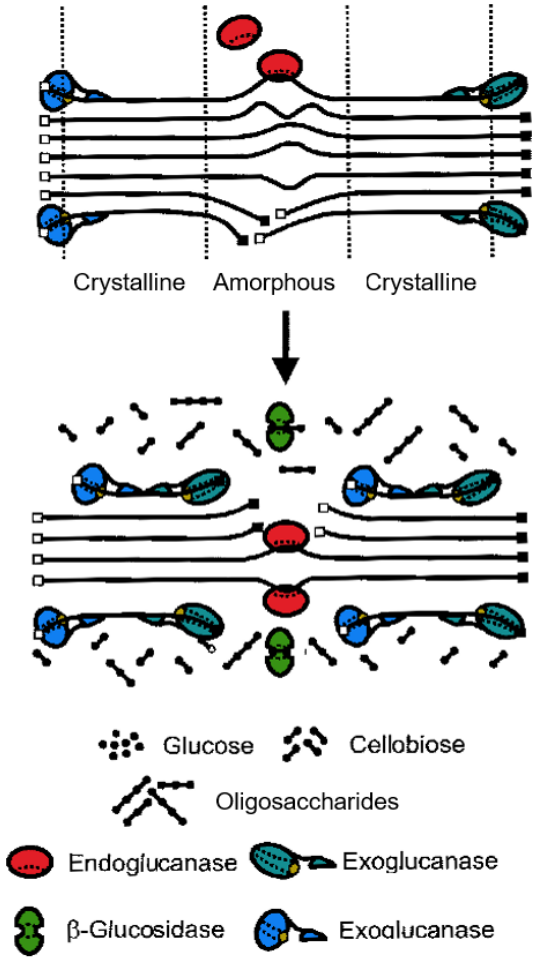

Figure 2.2: Schematic representation of the action of different types of cellulases on cellulose molecules. Adapted source: (Hardy 2016).

These type of enzymes are produced by a broad range of microorganisms which can be aerobic, anaerobic, mesophilic or thermophilic (Mojsov 2016). Between these the genera *Clostridium*, *Cellulomonas*, *Thermomonospora*, *Trichoderma*, and *Aspergillus* are the most studied and utilized in the industry as cellulases producers (Mojsov 2016). In particular the species *Trichoderma reesei* has gained a lot of attention in several branches of the industry and recently it has been widely investigated in the lignocellulosic bioethanol process because of its ability to produce an enzyme cocktail capable of performing the complete hydrolysis step (Druzhinina and Kubicek 2017).

2.7 *Trichoderma reesei*

2.7.1 History

Trichoderma reesei, anamorph of *Hypocrea jecorina*, is an aerobic mesophilic and filamentous fungus. Its biological characterization is presented in Table 2.1.

Table 2.1: Biological classification of *Trichoderma reesei*. Source: (Hardy 2016).

Kingdom	Fungi
Division	Ascomycota
Sub-division	Pezizomycotina
Class	Sordariomycetes
Sub-class	Hypocreomycetidae
Order	Hypocreales
Family	Hyproceaceae
Gender	Trichoderma

It was first isolated from Solomon Islands during World War II, due to its degradation of canvas and garments of the US army (Seidl et al. 2009). It was stored at the Natick Army Research Laboratories led by Mary Mandels and Elwyn T. Reese, the researcher who named it (Geng 2014).

The first strain to be studied was identified as QM6a (Bischof et al. 2016) and since then studies have been conducted on this species of fungus that revealed its great ability to segregate large amounts of hydrolytic enzymes, which are applied nowadays in several industries such as pharmaceutical, food, paper and biofuels (Bischof et al. 2016; Keshavarz and Khalesi 2016). The latter is where *T. reesei* has been used the most and gained more popularity, because of its significant power of production of cellulases (Keshavarz and Khalesi 2016), that allows the degradation of cellulose into sugars which can be then converted to bioethanol.

The use of *Trichoderma reesei* as cellulase producer obtained a lot of interest during the oil crisis in the 1970s when bioethanol processes from cellulose became economically attractive (Harman and Kubicek 1998). However enzyme production had elevated costs because of the low enzyme yields of the fungi strains that were available at the time, which hindered their economical use (Harman and Kubicek 1998).

Later with the evolution of genetic engineering technologies, witnessed for the past years, researchers have been able to develop a genomic map for its manipulation in order to create hyperproductive mutants from the strain QM6a with the purpose of increasing enzyme production (Bischof et al. 2016; Harman and Kubicek 1998).

2.7.2 *Trichoderma reesei* Morphology

Filamentous fungi, like *Trichoderma reesei*, begin their life cycle as conidia which then evolve into hyphae after germination (Etxebeste and Espeso 2016) . Hyphae are cylinders that grow by apical extension and are made up from multiple cells separated by septa (Harris 2008). Each extension of an apical compartment is associated to a mitosis cycle in which the separation of the nucleus is followed by the septa of the compartment (Ahamed and Vermette 2009).

The extension of the hyphae is performed by apical and lateral branching, as illustrated in Figure 2.3. The different branches merge together forming anastomosis (Etxebeste and Espeso 2016), that generate a complex network of interconnected cells called the mycelium (Harris 2008). The branching

of the hyphae can have two distinct objectives: enhance the surface area in order to increase nutrient capture and by the fusion of the hyphae the exchange of nutrients between cells and signals between different hyphae in the same colony of fungus (Harris 2008).

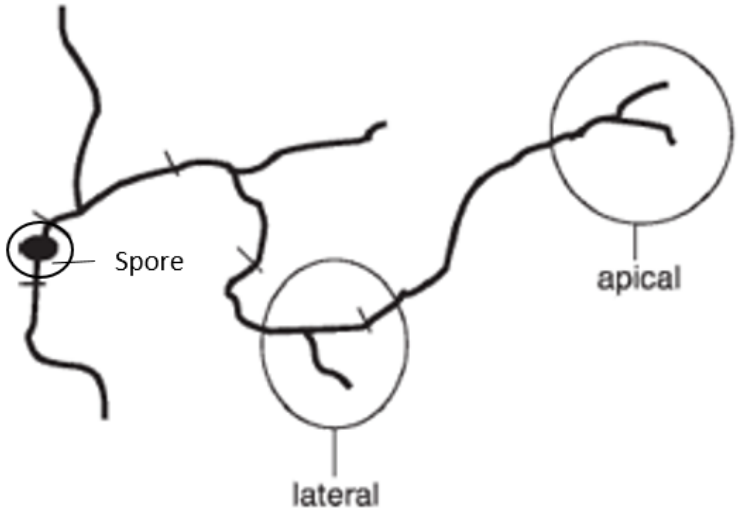

Figure 2.3: Schematic representation of a fungal hypha that presents lateral and apical branching behaviour. The oval black shape represents the spore and the stripes on the primary hyphae represent the septa. Adapted source: (Harris 2008).

The morphology of the fungus *T. reesei*, as others filamentous fungi, has an important impact on the fermentation broth rheology, affecting the gas-liquid mass transfer and thus the cellulase productivity (Gabelle et al. 2012b). With the growth of the mycelium the viscosity of the medium increases turning into a non-Newtonian mixture which becomes strongly shear thinning (Gabelle et al. 2012b; Marten et al. 1996). As the viscosity of the broth rises the mass transfer between the air and the liquid is more difficult, impacting the growth and production during the fermentation, since *T. reesei* is strictly aerobic (Marten et al. 1996; Gabelle et al. 2012b). An easy solution for this problem could be the increment of the stirrer rate or the gas flow rate (Gabelle et al. 2012b). Still none of the possibilities are desirable since they would imply an increase in operation and investment costs (Gabelle et al. 2012b). In addition, foaming problems and shear damage can occur when the impeller velocity and gas flow rate are increased (Gabelle et al. 2012b). So, in order to optimize the enzyme production it is necessary to establish the proper values for the agitation an aeration parameters to guarantee a suitable oxygen and nutrient transfer to the cells, without losing enzyme activity (Marten et al. 1996).

2.7.3 Protein Secretion in *T. reesei*

The secretion of proteins in *Trichoderma reesei*, as well as in another filamentous fungi, can occur either by the conventional route or by unconventional secretions (Chengcheng Li et al. 2019). In *T. reesei* the protein secretion usually happens through the first one, where finished synthesized proteins are transported to the endoplasmic-reticulum for folding, modification and subunit assembly. Then the proteins are transported to the Golgi complex by vesicles (Saloheimo and Pakula 2012; Chengcheng Li et al. 2019). In this organelle the proteins suffer further modifications and are again wrapped up in transport vesicles that can be forwarded to the vacuole, the Spitzenkörper or to the membrane for exocytosis (Saloheimo and Pakula 2012; Chengcheng Li et al. 2019).

The exocytosis process, in a fungus like *Trichoderma reesei*, occurs mainly at the ends of the growing hyphae since the Golgi and the endoplasmic-reticulum are very abundant in that area (Nevalainen and

Peterson 2014; Chengcheng Li et al. 2019). This phenomena is called apical secretion (Chengcheng Li et al. 2019). Despite that, the exocytosis has been noticed in other regions of the cells, like the septa (septal secretion) (Hayakawa et al. 2011) and in the lateral plasmatic membrane (Valkonen et al. 2007). The secretion mechanism in filamentous fungi is illustrated in Figure 2.4.

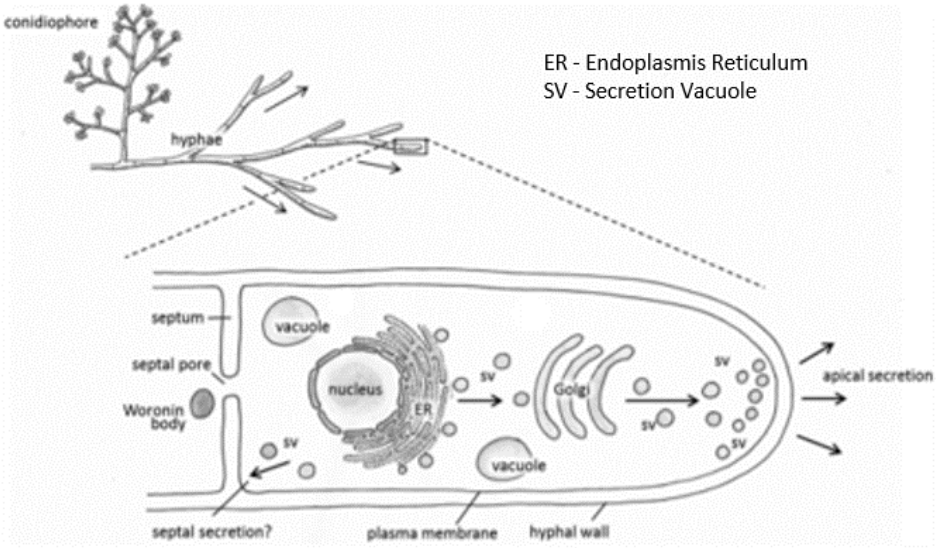

Figure 2.4: Schematic representation of the possible pathways for protein secretion in fungi. Adapted source: (Gonçalves Roque 2019).

Trichoderma reesei is able to produce several enzymes: two cellobiohydrolases (CBHI and CBHII), five endoglucanases (EGI, EGII, EGIII, EGIV and EGV) and two beta-glucosidases (BGLI and BGLII) (Kunamneni et al. 2014; Geng 2014). Beyond cellulase production, this species is also responsible for the release of hemicellulases like endoxylanases, XYNI and XYNII, and β-xylosidase, BXL1 (Geng 2014; Kunamneni et al. 2014).

2.7.4 Cellulase Biosynthesis in *Trichoderma reesei*

Like explained before, in order to decrease the costs associated with enzyme production it is imperative to enhance its production and activity. One way to do that is to improve the strain expression capacity through genetic engineering (Schmoll and Dattenböck 2016). In Figure 2.5 below are presented the several possibilities to improve the strain expression in filamentous fungi.

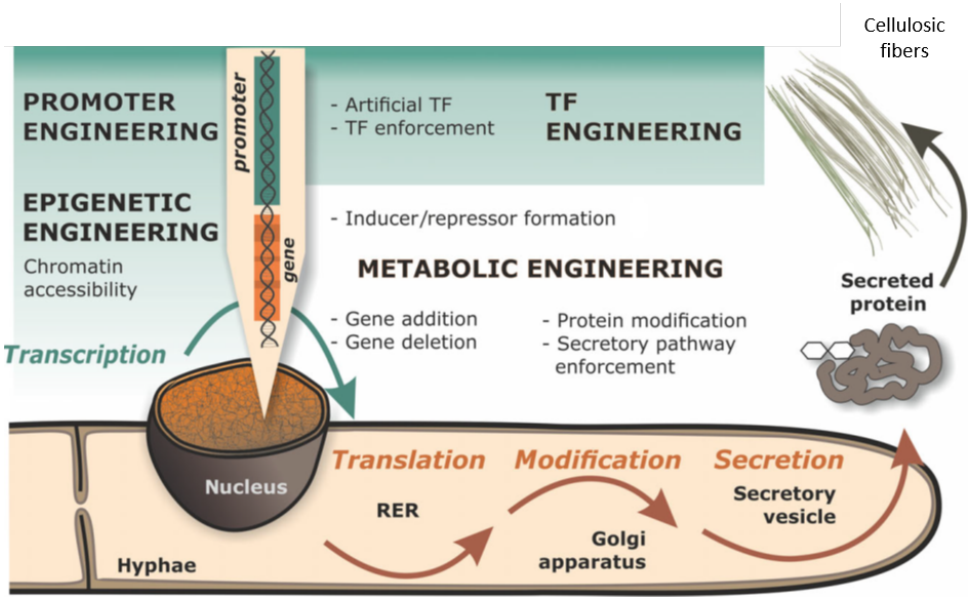

Figure 2.5: Genetic engineering strategies to improve Trichoderma reesei cellulase production. Abbreviations: TF – transcription factor, RER – rough endoplasmic reticulum. Adapted source: (Druzhinina and Kubicek 2017).

The expression of cellulases and some hemicellulases in *Trichoderma reesei* is induced by the growth on carbon sources like cellulose and some disaccharides such as lactose and sophorose (Druzhinina and Kubicek 2017; Schmoll and Dattenböck 2016). Consequently the cellulase expression can be enhanced by the manipulation of a small number of regulators that have influence in the expression of cellulases (Druzhinina and Kubicek 2017; Schmoll and Dattenböck 2016). For example, in *T. reesei* the promoter cbh1, responsible for the initiation of the transcription of the genes of cellobiohydrolases are induced by the presence of the mentioned sugars. Several hyperproductive strains of *T. reesei*, have a high expression of cbh1 (Schmoll and Dattenböck 2016). However, the increased concentration of D-glucose has a repressive effect on the cellulase gene expression because of the action of a carbon catabolite repressor protein CRE1 that binds to the promoters of the genes of cellulases preventing its transcription (Portnoy et al. 2011; Schmoll and Dattenböck 2016).

The fact that cellulase expression is regulated by the inducible promoters allows a production of proteins in two different steps: cell growth phase followed by an enzyme production step in which an inducer is added to the broth. Such inducer should be a cheap substance which does not have an impact on the cell physiology but has an effect on the expression of the gene that is regulated by its concentration (Schmoll and Dattenböck 2016). From the inducers previously presented, lactose is the most suitable option since it has the lowest cost and it is water soluble contrary to cellulose.

The lactose induction mechanism is regulated by three proteins that are essential for cellulase production (Zhang et al. 2019). The proteins are ACE3, XYR1 and Crt1 (Zhang et al. 2019). The Crt1 is a cellulase inducer transporter (Zhang et al. 2019). The XYR1 and ACE3 are both transcriptional activators (Druzhinina and Kubicek 2017). The first regulates cellulase and xylanase gene expression (Druzhinina and Kubicek 2017) and the second controls cellulase activity and lactose metabolism (Zhang et al. 2019). The interaction between these three regulators, represented in Figure 2.6, is responsible for controlling cellulase expression and lactose metabolism in *Trichoderma reesei* (Zhang et al. 2019).

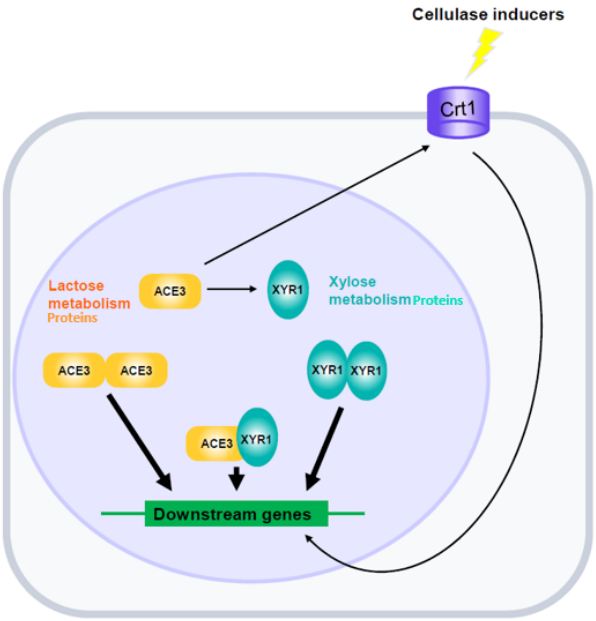

Figure 2.6: Gene regulation mechanism responsible for the cellulase induction. Adapted source: (Zhang et al. 2019).

The ACE3 protein, in the presence of lactose, can bind to the promoters of cellulase genes and also regulate *bgal* promoter that is responsible for the production of beta glucosidase, the enzyme responsible for the hydrolysis of lactose into glucose and galactose, since the first cannot be uptaken directly by the cells to be metabolized (Zhang et al. 2019). Additionally ACE3 interacts with Crt1 and XYR1 to regulate indirectly the cellulase production by forming heterodimers (Zhang et al. 2019). Also XYR1, in the presence of cellulase inducers like lactose, can bind to cellulase promoters in the form of homodimers to regulate its expression (Zhang et al. 2019).

2.7.5 *Trichoderma Reesei* Cultures

As already stated before, *Trichoderma reesei* has a great potential as a cellulase producer due to its great secretion capacity of different types of these enzymes. Because of this ability it has been widely used in the several branches of industry like in the second generation biofuels, due to its degradation capacity of lignocellulose. However the cost of the production of such protein metabolites is very high (Darabzadeh et al. 2019). Therefore scientists have been investigating the best way to optimize this fungus productivity through different forms of cultivation (Darabzadeh et al. 2019).

The production of cellulases by the fungus *T. reesei* can be carried out by two different types of cultures/fermentations: solid state fermentation (SSF) and submerged fermentation (SmF) (Hemansi et al. 2019).

The SSF procedure is performed in the absence or near absence of free water, but the substrate has to have the moisture required for the growth and metabolism of microorganisms, which grow attached to the solid substrate surface (Thomas et al. 2013). These conditions are similar to those where they can be found in the nature (Prado Barragán et al. 2016). This type of fermentation is accomplished in tray bioreactors, packed bed reactors or in rotary drum bioreactors (Hemansi et al. 2019).

The SmF is a process in which the growth of microorganisms takes place in a liquid medium where certain necessary nutrients and oxygen are dissolved in the broth, which ensures adequate heat and mass transfer (Doriya et al. 2016; Hemansi et al. 2019). This type of fermentation is normally carried out in stirred tank reactors, however airlift reactors and bubble columns have been also used to improve

the oxygen transfer to the liquid (Hemansi et al. 2019; Prado Barragán et al. 2016).

The SSF, compared with the SmF, has the advantages of being more economical, due to low operational costs and higher enzyme yield (Hemansi et al. 2019). Nevertheless, the SmF is more easily monitored and controlled which makes it easy to scale up, contrary to the SSF that can only be employed at small scales and so its achievable production is smaller compared to the SmF (Hemansi et al. 2019). This is why the SmF process is the one used in industry (Hemansi et al. 2019).

The SmF has different methods to be operated that are: batch, continuous, and fed-batch (Hemansi et al. 2019). In batch fermentations all the required components are present inside the reactor at the beginning of the operation and there are no inlet of nutrients or outlet of products until the end of the process (Hemansi et al. 2019). Only gases and pH buffers are supplied continuously during the operation (Hemansi et al. 2019). The continuous method is in contrast to the batch, since the nutrients and the cells are continuously fed to the reactor and removed alongside the products at the same flow rate, in order for the volume to stay constant (Hemansi et al. 2019). The fed batch mode of operation lies between the other two presented before (Hemansi et al. 2019). In this method, nutrients are fed to the reactor in intermittent regimen but there is no outlet of components during the process (Hemansi et al. 2019). From the three types of operation the fed-batch has an extra advantage of reducing the catabolite repression due to the inlet of substrate at different times which enables a control of the amount of substrate inside the reactor (Hemansi et al. 2019). This is especially important for the production of cellulases by *Trichoderma reesei* which is highly repressible by the concentration of glucose in the medium, as said before.

In Table 2.2 are presented examples of studies carried out with different types of operation of SmF for the production of cellulases by strains of *T. reesei*.

Table 2.2: Examples of studies about the production of cellulases by *Trichoderma reesei* with different operation methods of SmF.

***T. reesei* strain**	**Mode of operation**	**Substrate/ Inducer**	**Operation time (h)**	**Reactor volume (L)**	**Cellulase productivity (U L^{-1} h^{-1})**	**Reference**
Rut-C30	Batch	Cellulose	192	14	55	(Hendy et al. 1984)
C5	Batch	Lactose	185	4	31.55	(Chaudhuri and Sahai 1993)
C5	Continuous	Lactose	-	5	61.2	(Chaudhuri and Sahai 1993)
Rut-C30	Continuous	Cellulose	-	14	97	(Hendy et al. 1984)
Rut-C30	Fed-Batch	Cellulose	320	5	133	(Hendy et al. 1984)
QM 9414	Fed-Batch	Cellulose	180	5	20.6	(Ghose and Sahai 1979)

2.8 Modelling of *Trichoderma reesei* cultures for the production of cellulases

Due to the importance of cellulase production, as explained before, it is therefore necessary to understand, as much as possible, the biochemical processes underlying the growth and enzyme production of the fungi. With this knowledge it is possible to optimize the production of cellulases. The construction of mechanistic models that represent the behaviour of such cultures, has been shown to be a great instrument to help researchers to know better the physiology of the strains, since it can indicate the most promising lines of research giving rise to new experiments that reveal new biochemical mechanisms that increase the knowledge of the culture behaviour. Also it is possible to use models, that are a good representation of culture behaviour, for optimization, scale-up and process control, combined with engineering techniques. Because of this, many studies have been conducted for the past years to develop models that can be used to predict and mimic the production of cellulases by *Trichoderma reesei*.

There are several approaches to model the kinetics of microorganisms. Nielsen and Villadsen (1992) present a detailed review about such approaches where they explain the difference between unstructured and structured models regarding the modelling of the cell and the population.

Rakshit and Sahai (1991) formulated a semi-empirical model to describe the growth and cellulase production by *T. reesei* strain E-12 in batch fermentation with cellulose as substrate, and developed an optimal pH control strategy to enhance cellulase production. However, the substrate consumption was not taken into account and so the model did not consider the dependence of the cell growth on the substrate concentration.

Bader et al. (1993) developed a more detailed model for batch processes with the strain *T. reesei* RUT-C30 growing and producing cellulases on potato pulp as substrate. This model takes into account the differentiation of the substrate into amorphous and crystalline cellulose, as well as hemicellulose and some non-sugar components. It also contemplates physiological modifications in the cells that give a better description of the behaviour of the culture. Besides this, it takes into consideration the adsorption of the enzymes on the substrate with the subsequent hydrolysis into smaller sugars that are uptaken by the cells in order for them to grow. Additionally, it also differentiates the cellulases that are produced during the fermentation, namely endoglucanases and exoglucanases.

Velkovska et al. (1997) created a kinetic model based on that of Bader et al. (1993) for batch cultures of the same strain but with purified cellulose as a substrate. However, their strategy towards the enzyme production was more simplified since they considered that the enzyme composition was the same throughout the process assuming a global production of enzymes without differentiation. Also, morphological and physiological changes were taken into account during the growth of the fungi with a structured approach regarding the biomass and substrate reactivity parameters but unstructured concerning the intracellular phenomena. Moreover, it was verified that the adsorption of the enzymes on the substrate can be described by the Langmuir adsorption isotherm.

Tholudur et al. (1999) used a different method to develop their model that was applied to *Trichoderma reesei* RL-P37 cultures on soluble sugars as substrate, namely lactose and xylose, in batch fermentation. Instead of trying to represent the structure of the system at the cell and population levels, they used a neural network parameter function modelling in an attempt to improve the accuracy and predictability of the model. The neural network parameter function modelling can be seen as a "macro-modelling" technique because it only uses fundamental macroscopic material balances. However, the authors combined this method with fundamental process knowledge creating a hybrid model. However, this method has the disadvantage of not providing comprehension about the mechanisms that describe the system.

Muthuvelayudham and Viruthagiri (2006) modelled a *Trichoderma reesei* RUT- C30 culture on a mixed substrate medium (cellulose and lactose). They verified that a Logistic model and the Luedeking-Piret model were a good approach to obtain kinetic parameters for evaluation of the behaviour of the fermentation process. An artificial neural network was also successfully used as a modeling tool.

Lo et al. (2010) were the first to develop a model, as complete as the present thesis, for a continuous culture of *Trichoderma reesei* on a lactose as substrate and cellulase inducer. The model contemplates cell growth, substrate consumption, lactose hydrolysis and lactase and cellulase production. All of these features were successfully described by the mechanistic model. A Monod type equation was used to represent the specific growth rate and a modified Luedeking-Piret kinetics for the specific rates of lactase and cellulase production in which the first was growth dependent and the second growth independent. The authors also verified a diauxic growth behaviour of the microorganism with mixtures of glucose and galactose, that result from the hydrolysis of lactose, due to the catabolite repression of glucose on galactose, since the first was preferably consumed by the fungus. Such behaviour was also included in the model equations.

Bannari et al. (2012) applied CFD (computational fluid dynamics) calculations to an airlift bioreactor creating an innovative model for this type of cultures. The fermentation of *Trichoderma reesei* RUT-C30 was performed in fed batch mode with lactose and cellulose as substrates. The innovation that these authors brought with this study was the modeling of the kinetics of the culture together with the reactor performance which includes the description of the flow pattern and the mas transfer. This way the model was able to provide information about the distribution of oxygen, cellulose and shear stress during the entire fermentation. The two phase model contemplates several state of the art equations to describe the flow dynamics, mass transfer phenomena as well as the kinetics of the fungal metabolism.

Lastly Ma et al. (2013) developed a simple model, yet a complete one, for *Trichoderma reesei* batch cultivations with cellulose as substrate. The model was then applied to fed batch fermentations to enhance cellulase production by devising a feeding strategy. The construction of the model was carried out with the following assumptions: cellulose is the only limiting substrate; the composition of the cellulase cocktail was always the same; neglected inhibition by cellobiose and glucose due to small values of reducing sugars concentrations. A Monod kinetics was used to describe the growth and a modified Luedeking-Pieret was employed for the cellulose consumption. The cellulase activity was modeled in the same way as in Velkovska et al. (1997). The best feeding strategy that was utilized is the following: decreasing amounts of cellulose under intermittent feeding with an interval of 6 h. The strategy allowed an increase of 82,13% in cellulase activity when compared with the batch fermentation.

Chapter 3

Materials and methods

3.1 Experimental Results

To validate the performance of the model experimental results were used in both parts of this thesis. The experimental procedures carried out in the laboratory to obtain these data are explained below.

3.2 The Strain

The strain TR30060 was used in both sets of experiments. This strain is a descendant of CL847 strain that was genetically improved by the Biotechnology department of IFPEN in collaboration with the company PCAS Proteus (Longjumeau, France).

3.3 Experimental procedure used to the laboratory data with one reactor

For this set of experiments, which were named K1489, K1490, K1491, K1492, a 1.5 L bioreactor was used with an initial volume of liquid of 0.8L and the oxygen concentration in the liquid is fixed at 40% of dissolved oxygen saturation (DO). The batch phase was initiated with a glucose concentration of 30 g/L. During this step the temperature was kept constant at 27 ℃, the pH was controlled at 4.4 by the addition of an ammonia solution (5.5N) and the impeller rotation speed was 800 rpm. Then the fed batch started at 24 hours of cultivation for the K1489, K1491 and K1492 runs and at 48 hours for the K1490 run with a flow rate of 2 mL/h of a solution of lactose with a concentration of 210 g/L. For the K1491 run the fed batch substrate/inducer is composed by 25% lactose and 75% glucose at the same overall concentration. During the fed batch the temperature was 25 ℃, the pH was controlled at 4 by the addition of the same ammonia solution described above, and the impeller speed was 1000 rpm. Sampling was carried out to measure biomass and protein concentrations in the broth. In the Table 3.1 the conditions for each of the experiments mentioned are presented.

Table 3.1: Description of the conditions of the different experiments.

Experiment	Time of Fed Batch start (h)	Batch substrate	Fed Batch substrate
K1489	35	Glucose	Lactose
K1490	45	Glucose	Lactose
K1491	35	Glucose	75% Gluc + 25% Lact
K1492	35	Lactose	Lactose

3.4 Experimental procedure used to obtain the laboratory data with two reactors

In this part of the experimental work the effect of physicochemical heterogeneities introduced by scale-up on the behaviour of the fungus *Trichoderma reesei* was studied using a scale down approach that consisted on a "Bizone" system composed of two interconnected reactors, each characterized by different concentrations of dissolved oxygen, one of the reactors being operated as aerobic (DO=40%) and the other as anaerobic (DO = 0%). However, initially in the growth phase the experiment starts with only one reactor of 3.5 L of total volume with an initial volume of medium of 2.5 L. During this phase the temperature is kept constant at 27 ºC and the pH controlled at 4.8 through the addition of an ammonia solution (5.5 N) and the agitation speed is fixed at 800 rpm. The initial glucose concentration in the bioreactor is 30 g/L. It is considered that the growth phase is finished when the concentration of residual glucose in the medium is less than 5 g/L, which means that the fungus has consumed almost all of the sugar initially introduced. Then the production phase begins. This phase is carried out at 25 ºC for approximately 230 hours, with a pH regulated at 4.0 by injecting an ammonia solution at 5.5 N, and a stirring speed fixed at 1000 rpm. The fed-batch is operated by adding lactose at 210 g/L with a flow rate of 4 mL/h in order to maintain a residual sugar concentration close to zero. After the fed batch begins the dissolved oxygen is controlled at 40% by changing the oxygen content in the inlet gas and 96 hours after the start of the fed-batch, this aerobic bioreactor is connected to another bioreactor of 2.0 L of total volume, which is subsequently operated without aeration (under N_2 flushing), with 0.5 L of culture that was withdrawn from the aerobic reactor. The fermentation medium then circulates between the two bioreactors with a flow rate of 150 mL/min. The feeding with lactose is carried out only in the aerobic bioreactor. Two peristaltic pumps ensure the circulation of the broth between the two bioreactors throughout the production phase. Also an automated system controls the weight of the anaerobic reactor in order for the liquid volume to be kept at 0.5 L. Figure 3.1 shows the experimental setup in the configuration that was just described. In addition to the bizone experiment, another was carried out using this system that is the inverted bizone in which the reactor that is unaerated is the bigger one and the small one is aerated. In this case, lactose feeding was done on the small reactor, the aerated one.

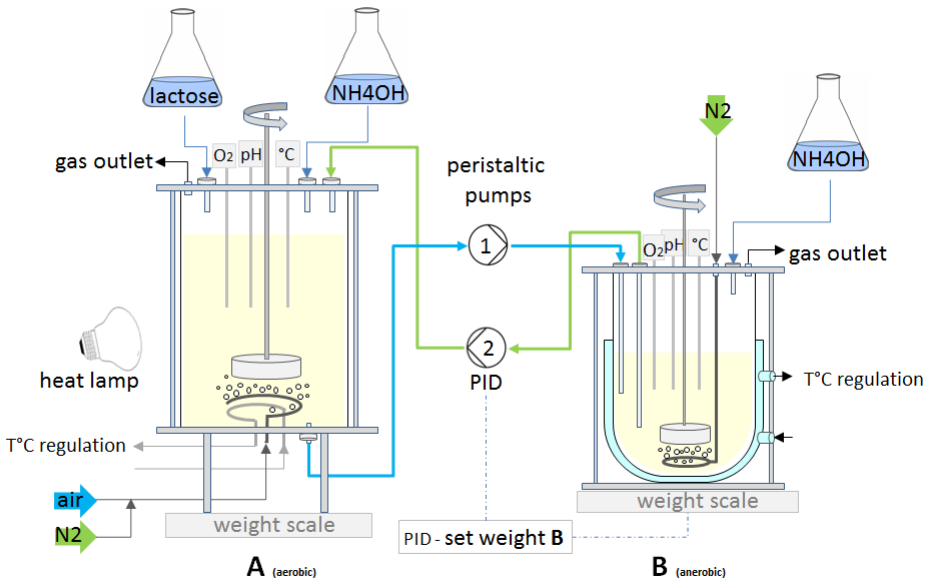

Figure 3.1: Experimental set up that was used in the laboratory to perform cultures of *Trichoderma reesei* to produce cellulases in conditions designed to study scale up problems like inefficient mixing that can lead to gradients of substrate concentration and zones with low dissolved oxygen levels.

3.5 IFPEN process for cellulase production by *Trichoderma reesei*

IFP Energies nouvelles (IFPEN) has developed an optimized process for the production of cellulases, in submerged fermentation in a stirred tank reactor, which includes two phases: a growth phase and a production phase (Figure 3.2). The growth phase is carried out in batch mode using an excess of glucose as a carbon source. From an industrial point of a view, this phase can be carried out in several stages in fermenters of increasing capacity, aiming to gradually increase the volume of culture until the production fermenter can be inoculated. The second phase is dedicated to the production of cellulases. Its operating mode is fed-batch, allowing the reactor to be fed with lactose at an optimal limiting flow rate to induce the secretion of cellulases by the fungus, and prevent its repression by the accumulation of glucose due to the hydrolysis of lactose. This is the process that was targeted for modeling also at IFPEN.

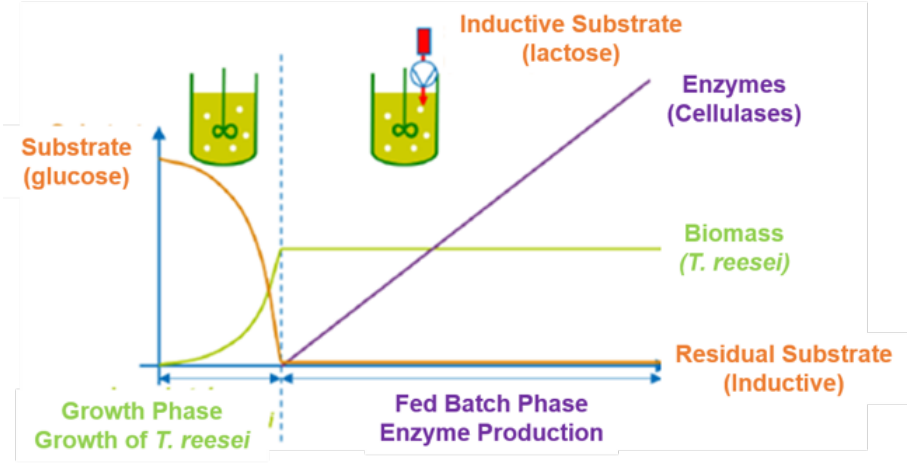

Figure 3.2: Schematic representation of the IFPEN protocol for cellulase production. Adapted source: (Jourdier 2012).

3.6 IFPEN growth and production model

IFPEN has also been developing a simple model to describe the behaviour of the cultures of *Trichoderma reesei* that are carried out following the previously explained strategy. The model considers that the cells are all equal, growing and producing cellulases at the same rate. It is also assuming the composition of the cellulase cocktail produced to be the same along time and so, there is no discrimination of the production of different cellulases. Additionally, the model does not discriminate between the different sugars involved in the process (glucose, galactose and lactose) considering that all are a common sugar substrate. This model contemplates the specific growth rate, production rate and consumption rates of oxygen and substrate.

Regarding the growth, it is described by a Monod type equation and a Michelis Menten term related with the dissolved oxygen available in the medium as presented in Equation A.16.

$$\mu = \frac{\mu_{\text{max}} \times [S]}{K_{\text{S}\mu} + [S]} \times \frac{[O_2]}{K_{\text{O}_{2\mu}} + [O_2]} \tag{3.1}$$

The μ_{max} represents the maximum growth rate at which the cells can grow and the constants $K_{s\mu}$ and $K_{O_{2\mu}}$ are the growth half saturation constants related with sugar and oxygen respectively. The [S] and the $[O_2]$ represent the substrate and oxygen concentrations, respectively.

The specific production rate takes into account the inhibition by the biomass and substrate due to the increase of the first during the growth phase and the higher concentrations of sugar present. It also varies according to Michaelis-Menten terms for oxygen and substrate as presented in Equation A.17:

$$q_{\text{p}} = \left(\frac{q_{\text{pmax}} - q_{\text{pmin}}}{1 + \frac{[X]}{K_{\text{iXP}}}} + q_{\text{pmin}}\right) \times \frac{[S]}{K_{\text{SP}} + [S]} \times \frac{[O_2]}{K_{\text{O}_2\text{P}} + [O_2]} \times \frac{K_{\text{iSP}}}{K_{\text{iSP}} + [S]} \tag{3.2}$$

The q_{pmax} represents the specific maximum theoretical production rate. The q_{pmin} is the specific theoretical minimum production rate. The constants K_{iXP} and K_{iSP} represent the inhibition of production by the biomass and substrate, respectively. The constants K_{SP} and K_{O_2P} are the production half saturation constants related with sugar and oxygen, respectively. The [X] represents the biomass concentration.

Both the consumption rates of oxygen and substrate contemplate the amount that it is spent for the growth, the production and the maintenance of the cells as described in the Equations A.19 and A.20 below:

$$q_{\text{s}} = \frac{\mu}{Y_{\text{x/s}}} + \frac{q_{\text{p}}}{Y_{\text{p/s}}} + m_{\text{s}} \tag{3.3}$$

$$q_{\text{O}_2} = \frac{\mu}{Y_{\text{x/O}_2}} + \frac{q_{\text{p}}}{Y_{\text{p/O}_2}} + {Y_{\text{O}_2/\text{s}}}^{\text{m}} \times m_{\text{s}} \tag{3.4}$$

The $Y_{x/s}$ and $Y_{p/s}$ represent the yield of biomass and enzyme on substrate, respectively. The m_s represents the specific rate of consumption of substrate for the cells maintenance. The Y_{x/O_2} and Y_{p/O_2} represent the yield of biomass and enzyme on oxygen, respectively. Finally the ${Y_{O_2/s}}^m$ represent the oxygen yield on substrate in maintenance reaction which is different depending on the sugar that is fed to the culture, meaning that there are two values for this variable: one for glucose and another for lactose.

The values for each parameter were obtained from the report "Modèle de production d'enzymes 2019" from Romain Rousset and are presented in the Table 3.2 below. The values of q_{pmax} and q_{pmin} presented here and on every place in this thesis (identified with "*") are normalized on the basis of their original value ranges, for confidentiality reasons. Protein concentration values in graphs are also given using a normalized scale.

Table 3.2: Values of the Kinetic and yield parameters of the existing model.

Parameter	Value	Units
μ_{max}	0.07 – 0.1	h^{-1}
$K_{s\mu}$	1	gS/L
$K_{O_{2\mu}}$	0.0001	gO_2/L
q_{pmax}^{*}	80 - 100	%
q_{pmin}^{*}	40	%
K_{iXP}	30	gX/L
K_{iSP}	10	gS/L
K_{SP}	0.001	gS/L
K_{O_2P}	0.0001	gO_2/L
$Y_{x/s}$	0.5	gX/gS
$Y_{p/s}$	0.5	gP/gS
m_s	0.01	gS/(gX.h)
Y_{x/O_2}	1.04	gX/gO_2
Y_{p/O_2}	1.22	gP/gO_2
$Y_{O_2/gluc}^{m}$	1.07	gO_2/gS
$Y_{O_2/lac}^{m}$	1.12	gO_2/gS

3.7 Mass Balance Equations

To develop the mass balances, the two operation modes were considered, the batch and fed-batch. So a general equation for all the components can be written to model the liquid phase, as presented below:

$$\frac{dm_i}{dt} = r_i V_L + (Q_{i_{in}} - Q_{i_{out}}) \tag{3.5}$$

In which dm_i/dt represents the variation of mass of i during time (g/h), r_i is the rate of i [g/(L.h)], the V_L is the volume of liquid (L), $Q_{i_{in}}$ is the inlet flow rate of i (g/h) and $Q_{i_{out}}$ is the outlet flow rate of i (g/h).

Taking into account that there is no biomass or enzymes entering and leaving the reactor, and there is only inlet of sugar during the fed-batch and the oxygen that is transferred from the gas phase, the air, to the liquid phase is used by the cells at the same rate, the equations for the concentration dynamics of each component are presented below.

$$\frac{dm_i}{dt} = \frac{d[i]V_L}{dt} = [i]\frac{dV_L}{dt} + V_L\frac{d[i]}{dt} \rightleftharpoons \frac{d[i]}{dt} = \frac{1}{V_L}\frac{dm_i}{dt} - \frac{[i]}{V_L}\frac{dV_L}{dt} \tag{3.6}$$

$$\frac{d[X]}{dt} = \mu[X] - \frac{[X]}{V_L}\Delta Q_v \tag{3.7}$$

$$\frac{d[P]}{dt} = q_p[P] - \frac{[P]}{V_L}\Delta Q_v \tag{3.8}$$

$$\frac{d[S]}{dt} = -q_s[X] + \frac{Q_{fb}[S_{fb}] - [S]\Delta Q_v}{V_L} \tag{3.9}$$

$$\frac{d[O_2]}{dt} = -q_{O_2}[O_2] + k_L a([O_2]^{*} - [O_2]) - \frac{[O_2]}{V_L}\Delta Q_v \tag{3.10}$$

$$\Delta Q_{\text{v}} = \frac{V_{\text{L}}}{dt} = Q_{\text{base}} + Q_{\text{fb}} - Q_{\text{evp}} \tag{3.11}$$

Notice that the $q_i=r_i/[i]$ (gi/gX/h). The i represents for the S, P and O_2.

The [P] represents the concentration of proteins or enzymes. The $[O_2]^*$ represents the concentration of oxygen at equilibrium with the gas phase. The $[S_{fb}]$ represents the lactose concentration of the solution that is fed to the reactor during the production phase. The ΔQ_v represents the variation of the volume of liquid inside the reactor, the Q_{base} represents the ammonia flow rate that was fed to the reactor, the Q_{fb} represents the substrate inducer (lactose) solution flow rate that is fed to the reactor during the production phase and the Q_{evp} is the amount of water that is lost through evaporation by the outlet of air in the unit time. The first two flow rates are known from the laboratory data, but the last one was calculated by doing a mass balance to the water in the gas phase in the reactor, as demonstrated below in Equation 3.12:

$$Q_{\text{air, in}} H_{\text{a, in}} + Q_{\text{evp}} = Q_{\text{air, out}} H_{\text{a, out}} \tag{3.12}$$

The $Q_{air,\ in}$ and the $Q_{air,\ out}$ represent the air flow rate at the inlet of the reactor and outlet, respectively. The inlet air flow rate is known and the outlet is assumed to be equal to it. The $H_{a,\ in}$ and the $H_{a,\ out}$ are the absolute humidity at the inlet and outlet of the reactor, respectively. To simplify the calculations, it was assumed that the air at the inlet is dry which means that the inlet humidity of the air is zero. The outlet humidity of the air was calculated by the Equation 3.13:

$$H_{\text{a, out}} = \frac{Pi}{P - Pi} \tag{3.13}$$

The Pi represents the partial pressure of water and the P the total pressure inside the reactor that is taken as 1 atm. It was also assumed that the air comes out water saturated, meaning that the relative humidity is 100% and that the Pi it is equal to the vapour pressure of water (P_v) at the operational temperature. Therefor the Pi is replaced by Pv, vapour pressure, in the equation 3.13. The vapour pressure was obtained from the NIST website for a temperature of 25 ºC. Note that this humidity is define in molar ratio so it was necessary to change to mass units using the molar masses of the air and water that are 28,96 g/mol and 18,02 g/mol, respectively. Also the air flow rate was converted from volumetric units to mass units considering the air as an ideal gas. In Table 3.3 the values of all parameters included in this calculation are presented for the conditions used in the first part of the results (1 reactor system) and for the conditions used in the second part of the results (2 reactors system with two different configurations: bizone and inverted bizone). Regarding the setup employed in the second part of the results, the evaporation of water in the anaerobic reactor was calculated assuming that the nitrogen sparged into it has the same psychometric properties of the air.

Table 3.3: Values of the operational flow rates and psychometric parameters used in the process models.

Parameter	Value	Units
$Q_{air,\ in}$	0.3	L/min
$Q_{air,\ in}$ bizone aerobic	0.08	L/min
$Q_{air,\ in}$ bizone anaerobic	0.25	L/min
$Q_{air,\ in}$ inv. bizone aerobic	0.25	L/min
$Q_{air,\ in}$ inv. bizone anaerobic	0.25	L/min
P_v	23.75	mmHg
$H_{a,\ out}$	0.032	mol H_2O/mol Air
Q_{evp}	$1.53x10^{-7}$	L/s
Q_{evp} bizone aerobic	$3.17x10^{-8}$	L/s
Q_{evp} bizone anaerobic	$9.57x10^{-8}$	L/s
Q_{evp} inv. bizone aerobic	$5.96x10^{-8}$	L/s
Q_{evp} inv. bizone anaerobic	$9.57x10^{-8}$	L/s

For the second part of this thesis it was necessary to include a term in each mass balance for each component to account for the recirculation lines between the two reactors. This term has the following construction: $Q_{r\ 1\text{-}2}[i]_1$- $Q_{r\ 2\text{-}1}[i]_2$. The $Q_{r\ 1\text{-}2}$ is the flow rate that comes from reactor 1 to reactor 2 and the $[i]_1$ is the concentration of the component in the reactor 1.The other variables in the term follow the same logic. This term is an example for the reactor 2 mass balances. For the reactor 1 the term is written the other way around. The full set of equations used for the two reactor system are presented in the Appendix A.

It was also necessary to model the gas phase in order to infer the variation of the concentration of oxygen in the liquid phase. To do that it was necessary to do a mass balance to the oxygen in the gas phase to then calculate the molar fraction of oxygen in the gas phase that will affect the oxygen concentration in the equilibrium liquid according to Henry's Law and consequently the OTR (oxygen transfer rate) variation during the fermentation. These calculations were done by knowing the inlet conditions of the air and its flow rate which were then used to calculate the oxygen and nitrogen inlet flow rates assuming the air as an ideal gas and that its molar composition is 21% of O_2 and 79% of N_2. The equations that represent the explanation given above are presented below:

$$\frac{d[O_2]_{\text{gas}}}{dt} = \frac{Q_{O_{2_{\text{in}}}} - Q_{O_{2_{\text{out}}}} - OTR \times V_L}{V_{\text{gas}}} \tag{3.14}$$

$$f_{O_2} = \frac{[O_2]_{\text{gas}}}{32} \times \frac{RT}{P} \times 1000 \tag{3.15}$$

$$K_H = \frac{[O_2]^*}{pO_2} \tag{3.16}$$

$$OTR = k_L a(K_H \times f_{O_2} \times P \times 32 - [O_2]) \tag{3.17}$$

$$Q_{O_{2_{\text{out}}}} = Q_{N_2} \frac{1 - f_{O_2}}{f_{O_2}} \tag{3.18}$$

The R, represents the ideal gas constant, the T represents the absolute temperature of operation and the K_H represents the Henry's law constant for oxygen that has the value of 0.0013 mol/(L.atm) at

25 ℃ obtained from the NEBIST website. The $[O_2]_{gas}$ represents the concentration of oxygen in the gas phase. The $Q_{O_{2_{in}}}$ and the $Q_{O_{2_{out}}}$ represent the inlet and outlet flow rate of oxygen in the reactor. The V_{gas} is the volume of gas inside the reactor. The f_{O_2} is the molar fraction of oxygen in the air. The Q_{N_2} is the inlet flow rate of nitrogen in the reactor.

To solve the differential equations, the Euler method was used, by giving initial values to the variables. This method, is an explicit one, which means that the values of the variables are calculated from the values from the previous time step. All the modelling calculations were implemented in Virtual Basic (VBA) language from Excel software package.

3.8 k_La and Hold-up Calculations

The values of the partial mass transfer coefficient of oxygen (k_La) and the hold-up of gas inside the reactors were calculated for the experiments with the setup of two reactors in order to model the gas phase and the transfer of oxygen from the air to the liquid. These constants were calculated for the conditions of the bizone configuration and the inverted bizone configuration. For the modelling work with the data that was obtained with one reactor, the value of the k_La was considered to be 0.1 s^{-1} and the hold-up parameter was not calculated, because the gas phase was not taken into account for the calculations in that part and, the oxygen concentration in the liquid phase was set constant at 40% of saturation as it was done in the laboratory.

The calculations of these variables were done according to the explanation given by Cappello et al. (2020), and are presented below in the following equations.

It begins with the calculation of the shear rate, for bioreactors smaller than 5 m^3, through the Metzner & Otto correlation, as presented in Equation 3.19.

$$\dot{\gamma} = 11.5N \tag{3.19}$$

The N represents the stirring rate of the impeller.

Then the apparent viscosity was calculated by Equation 3.20.

$$\mu_{app} = K\dot{\gamma}^{n-1} \tag{3.20}$$

The K is the consistency index ($Pa.s^n$) and the n the flow index.Both are parameters that define the rheology of the broth that varies during the fermentation. As these calculations were only done for the second part of the results and in this part only the production phase was taken into account (further explanation about this is given in the presentation of the second part results), these parameters were calculated for that step of the process. Therefore the n is equal to 0.2 and the K is calculated according to Equation 3.21:

$$K = 0.003[X] \tag{3.21}$$

With the [X] in gX/L. Then it was required to calculate the value of Pg/V that is the input of power per cubic meter in the reactor. Pg is defined by the Equation 3.22:

$$Pg = RPD \times Pu + Pa \tag{3.22}$$

In which RPD is the relative power demand and it is obtained by Equation 3.23. The Pu is the stirring power required if there is no aeration. The Pa is the power delivered by the injection of gas at the bottom

of the reactor.

$$RPD = max[RPD_{lim}, exp(-15.36{N_p}^{0.16}{Q_G}^{0.62}Td^{-1.7}(D/Td)^{0.51})] \tag{3.23}$$

According to Gabelle (2012a) the value of RPD_{lim} is 0.33. The N_p is the power number of the impeller, D is the impeller diameter, Td is the reactor diameter and the Q_G is the gas flow rate.

Then the Pa and the Pu were calculated by the Equations 3.24 and 3.25, respectively:

$$Pa = \rho L.g.V_{sg} \tag{3.24}$$

$$Pu = \rho L.Np.N^3.D^5 \tag{3.25}$$

The V_{sg} represents the gas superficial velocity, the ρL represents the liquid density that we considered to be mostly water and so the value given was 1000 kg/m^3 and the g represents the gravity acceleration that has the value of 9.8 m/s^2.

Finally, with the following correlation, represented by the Equation 3.26, the k_La and the gas hold up (α_G) were obtained.

$$Z(\equiv \alpha_G, k_La) = c_1(Pg/V)^{c_2}{V_{sg}}^{c_3}{\mu_{app}}^{c_4} \tag{3.26}$$

In the Table 3.4 the values of the constants c_1, c_2, c_3 and c_4 are presented for both the k_La and the hold-up.

Table 3.4: Values of the constants that were used to calculate the k_La and the hold-up.

Constant	**k_La (s^{-1})**	**Hold up**
c_1	0.000586	0.042
c_2	0.45	0.32
c_3	0.18	0.44
c_4	-0.48	-0.07

In Table 3.5 the values of the parameters needed to calculate the k_La and the hold-up are presented.

Table 3.5: Values of the Parameters used in the k_La and hold-up calculations.

Parameter	**Big Reactor**	**Small Reactor**
N (rpm)	1000	1000
Np	2	2
D (m)	0.08	0.055
Td (m)	0.16	0.11

In Table 3.6 below the values of k_La and hold-up obtained for both reactors in both configurations (bizone and inverted bizone) are presented.

Table 3.6: Values of $K_L a$ and hold up that were calculated for both reactors for the bizone and inverted bizone configurations.

Parameter	Big Reactor	Small Reactor
$k_L a$ bizone (s^{-1})	0.11	0.18
$k_L a$ inv. bizone (s^{-1})	0.11	0.14
Hold-up bizone	0.018	0.046
Hold-up inv. bizone	0.029	0.045

3.9 Additional considerations taken into account

During the entire work it was considered that the systems were perfectly mixed which means that it was considered that all the elements of volume have the same residence time in the bizone and inverted bizone configurations. As a final adjustment to the model, it was verified if this assumption led to results that were very far from those of the case where the reactor has a behaviour according to a residence time distribution that is represented by Equation 3.27:

$$E(t) = \frac{1}{\theta} e^{-t/\theta} \tag{3.27}$$

The E(t) accounts for the residence time distribution, the θ represents the average residence time and the t represents all residence time values theoretically possible.

Chapter 4

Results and discussion

4.1 First Part – Loss of Biomass

In this part of the thesis the objective is to model the result of 4 experiments with different fed batch compositions and if possible, try to come up with a relation between the changes in the production step of the experiments and the kinetic parameter values, that best fit the experimental results. In order to have a good fit of the experimental results and a reliable one it is important to guarantee an accurate prediction of the biomass evolution since the amount of proteins/enzymes produced depends on the biomass. if the model does not predict correctly the cells concentration the protein evolution given by the model will not be a realistic one.

As it can be seen in Figure 4.1 below, the biomass concentration starts to fall between approximately 50 and 70 hours for all the different experiments, which means that there is a loss of biomass. Initially the model was used to try to predict these results with the objective of assessing if the employed kinetic equation is good enough to explain the experimental results. The result of this attempt is presented in Figure 4.2 bellow, for one culture as an example and employing the initial model presented before in Chapter 3. It is important to note that the parameters used for all the simulations in this part were those presented in Table 3.2. The only constants that have different values between simulations are the μ_{max} and the q_{pmax} that were changed in order to obtain the best fit possible of the model to the experimental results. The values of these parameters that were used in the results in the Figure 4.2 are presented in Table 4.1.

Table 4.1: New values of μ_{max} and q_{pmax}.

Parameter	Value	Units
μ_{max}	0.08	h^{-1}
q_{pmax}^{*}	92	%

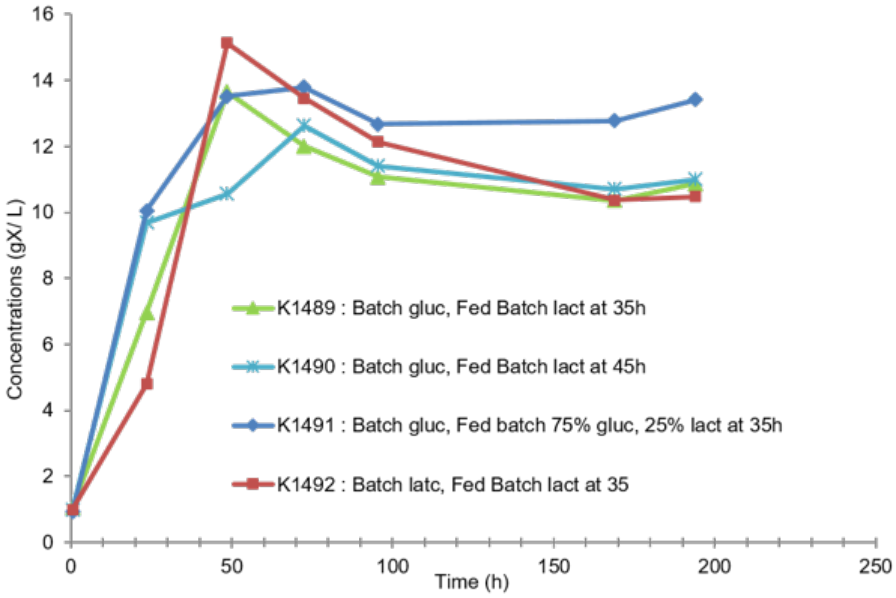

Figure 4.1: Experimental results of biomass concentration of four cultures with different fed batch compositions.gluc - glucose, lact - lactose

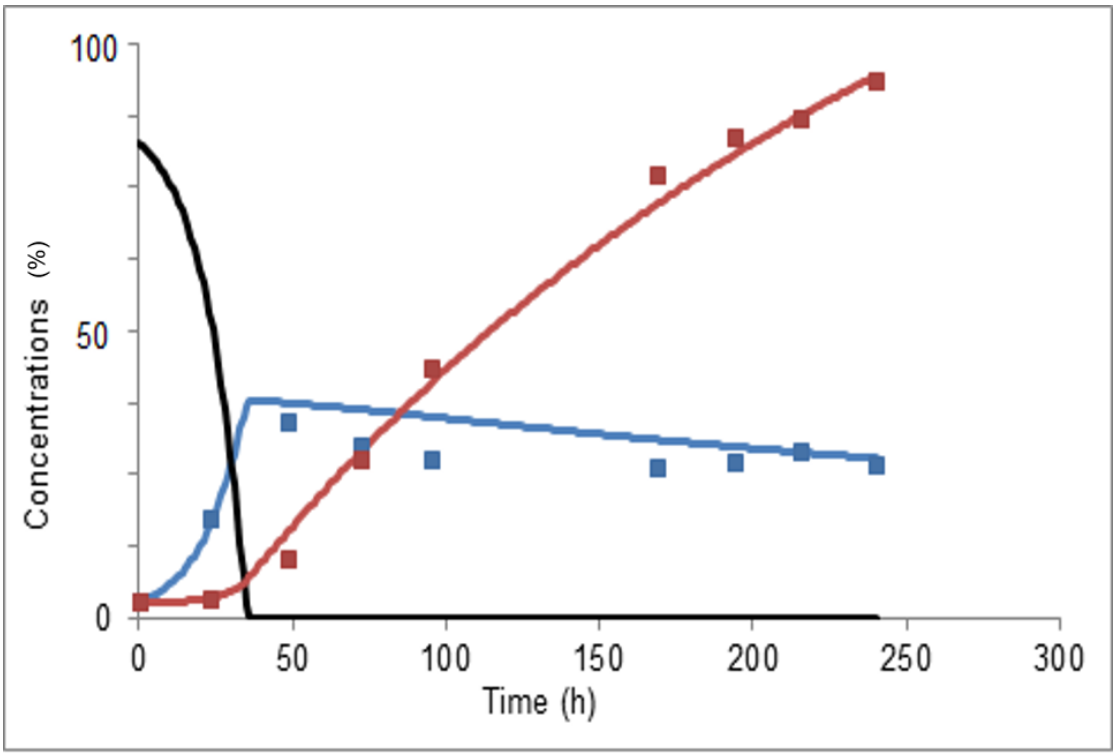

Figure 4.2: Results from the initial model for the culture K1489 (Batch gluc, Fed Batch Lact at 35 h), in which the marker ■ represents the experimental points of Biomass concentration and the ■ represents the experimental points of Protein concentration. The — represents the model prediction for the biomass concentration, the — represents the model prediction for the proteins concentrations and the — represents the model predictions for the substrate concentration.

By analysing the results in Figure 4.2 it can be seen that the model does not explain well the loss of biomass since the reason for the blue line (biomass concentration) to decline is merely the effect of dilution. Since the biomass is not well predicted the model results for the proteins cannot be trusted.

So from this point forward it was thought to implement a new mechanism in the model to improve the modelling of these cultures and try to come up with a reasonable relation between the kinetic parameters and the different fed batch compositions that were used for each experiment.

The biomass concentration starts to decline when the glucose is close to zero and so there is a change in the medium conditions since the fed batch has already started and the lactose is being fed to the reactor. So in this time gap the cells are starting to become aware of this change and adapting to the new conditions. It is thought that during this adaptation the fungus consumes the reserves of lipids, that were accumulated during the growth phase when there is excess of sugar, to produce proteins. This only happens until the cells are able to change the metabolism towards the hydrolysis of the lactose to obtain glucose and galactose that can be directly up taken by the cells. Therefore it was considered the following reaction, presented in Equation 4.1 to represent this lipid consumption process.

$$X \rightarrow P \tag{4.1}$$

Of course the real process of production of enzymes from lipids is much more complex due to the different steps that are required and the numerous intermediary molecules involved. Considering that this transformation is a first order reaction, its rate is presented in Equation 4.2 below.

$$-r = K \times [X] \tag{4.2}$$

Where K is obtained by the following Equation 4.3:

$$K = k \times (q_{\text{pmax}} \times \frac{[O_2]}{[O_2] + K_{\text{O}_2\text{p}}} - q_{\text{p}}) \tag{4.3}$$

The q_{pmax} is multiplied by a Monod type oxygen dependence term, since the value of this parameter will never be achieved because it is set in conditions where the concentration of oxygen in the broth is at saturation. So this multiplication gives a new value for the specific rate of protein production that can be reached during the fermentation, that is a more realistic value than q_{pmax}. The reaction constant was assumed to be proportional to the difference between the adjusted q_{pmax} and q_p since, when the biomass starts to decline the q_p is smaller than the adjusted q_{pmax} but, as the biomass concentration continues to decrease the value of q_p approaches the adjusted q_{pmax} value until the difference becomes zero and the lipid consumption mechanism stops to be active by itself. So what happens is that the biomass concentrations adapts to the new feed flow rate of substrate, that is inputted when the fed batch phase starts, in order to achieve the maximum production of enzymes.

With this new addition to the model the equations for the balances of biomass and proteins will gain a new term that will be equal to Equation 4.2 times the time step for both biomass and proteins. For the latter, it will also be necessary to divide by the yield coefficient $Y_{x/p}$ that represents the grams of biomass consumed to produce one gram of proteins. As the reaction suggest this new term will be subtracted from the previous balance equation for the biomass and of course will be added to the equation for the proteins. The new Equations 4.4 and 4.5 for these two balances are presented below.

$$\frac{d[X]}{dt} = \mu[X] - \frac{[X]}{V_{\text{L}}}\Delta Q_{\text{v}} - k(q_{\text{pmax}} \times \frac{[O_2]}{[O_2] + K_{\text{O}_2\text{p}}} - q_{\text{p}})[X] \tag{4.4}$$

$$\frac{d[P]}{dt} = q_{\text{p}}[P] - \frac{[P]}{V_{\text{L}}}\Delta Q_{\text{v}} - \frac{k}{Y_{\text{x/p}}}(q_{\text{pmax}} \times \frac{[O_2]}{[O_2] + K_{\text{O}_2\text{p}}} - q_{\text{p}})[X] \tag{4.5}$$

This new theory was implemented in such way that is only activated when the fed batch begins and when the sugar concentration is below 0.1 g/L in order to represent the adaptation of the culture to the new conditions, meaning a change in the type of substrate available and its feeding flow rate, as

explained above in this chapter. In Figure 4.3 below the modelling results for the K1489 culture, the same presented in Figure 4.2 but now with the new mechanism, are presented. This representation was obtained after finding out the set of values of k and $Y_{x/p}$ that best describe all the four experimental results. The values for these new parameters are presented below in Table 4.2. Note that the other parameters values for the results shown in Figure 4.3 are the same as presented in the Tables 3.2 and 4.1.

Table 4.2: Values of the parameters for the new mechanism.

Parameter	Value	Units
k	2.1	gX/gP
$Y_{x/p}$	1.73	gX/gP

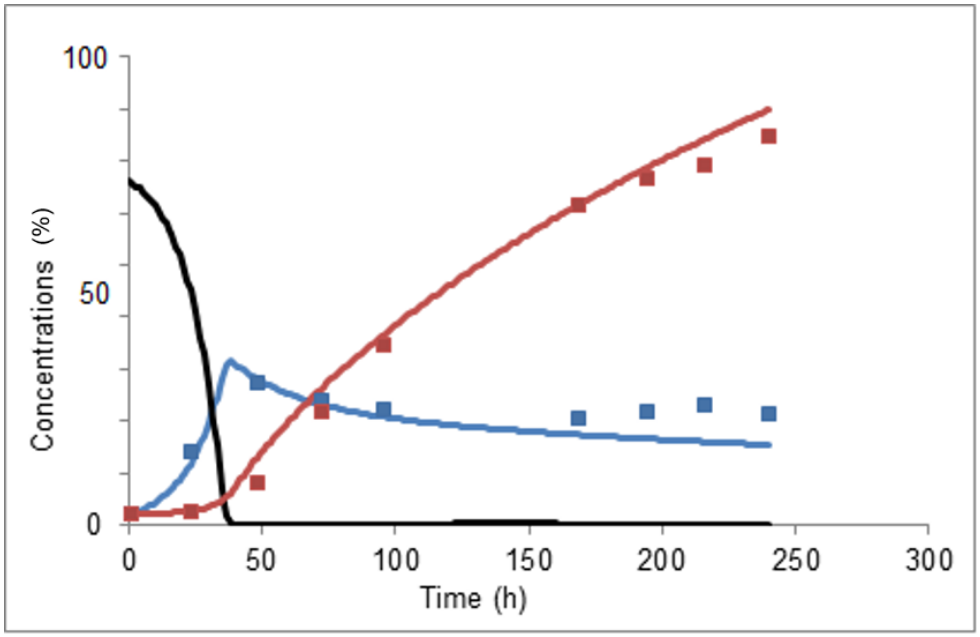

Figure 4.3: Results from the modified model for the culture K1489 (Batch gluc, Fed Batch Lact at 35 h), in which the marker ■ represents the experimental points of Biomass concentration and the ■ represents the experimental points of Protein concentration. The — represents the model prediction for the biomass concentration, the — represents the model prediction for the proteins concentrations and the — represents the model predictions for the substrate concentration.

With these results it is possible to see that the implementation of the new mechanism to represent the loss of biomass was successful since the model has a good prediction of the biomass concentration at the initial points of the production phase. However, what happens now is that the final points of the culture are not well explained by the improved model because the biomass concentration continuously decreases until the end of the fermentation, deviating from the experimental values, and the proteins concentration values are a little bit over predicted at the end. The reason why this happened is that the value of q_p does not reach the value of the adjusted q_{pmax} as it was supposed to. It is very close but never exactly the same, which prevents the lipid consumption mechanism from deactivating by itself and therefore the biomass concentration continues to decrease due to a residual contribution from this mechanism. This is not correct according to the theory that was thought since the idea was to consider a reserve of lipids that is then used at the start of the production phase, but this reserve has to run out at some point and this is not happening according to the modelling results presented.

So now it is necessary to improve the prediction of the final points of the concentration values in the

cultures. To solve this issue, several ideas were tried but only one was successful. This idea is based on the consideration of an aging of the culture which means that the cells grow older with time and because of that their metabolism will slow down. To represent this phenomenon, the q_{pmax} value was set to decrease following a linear function with time. With this new addition a new parameter was introduced in the model which is the fraction of decline (loss) of q_{pmax} during the fermentation. After doing some trials including the new model with the aging, a common set of parameters is proposed to model all the culture experiments with a maximum error of 20% for the experimental points. In Figures 4.4, 4.5, 4.6 and 4.7 below the modelling results, with the same parameter values, are presented for all the cultures. The values of the parameters are presented in Table 4.3 below. Note that the values of the variables regarding the new lipid consumption mechanism are the same as presented before in Table 4.2.

Table 4.3: Values of the variables that were used to model the four experimental runs including the aging effect

Parameter	Value	Units
q_{pmax}^{*}	88	%
μ_{max} (K1489,K1491)	0.085	h^{-1}
μ_{max} (K1490)	0.065	h^{-1}
μ_{max} (K1492)	0.07	h^{-1}
Loss of q_{pmax}	31	%

The value of μ_{max} was changed depending on the experimental in order to obtain the best fit possible of the model to the experimental points.

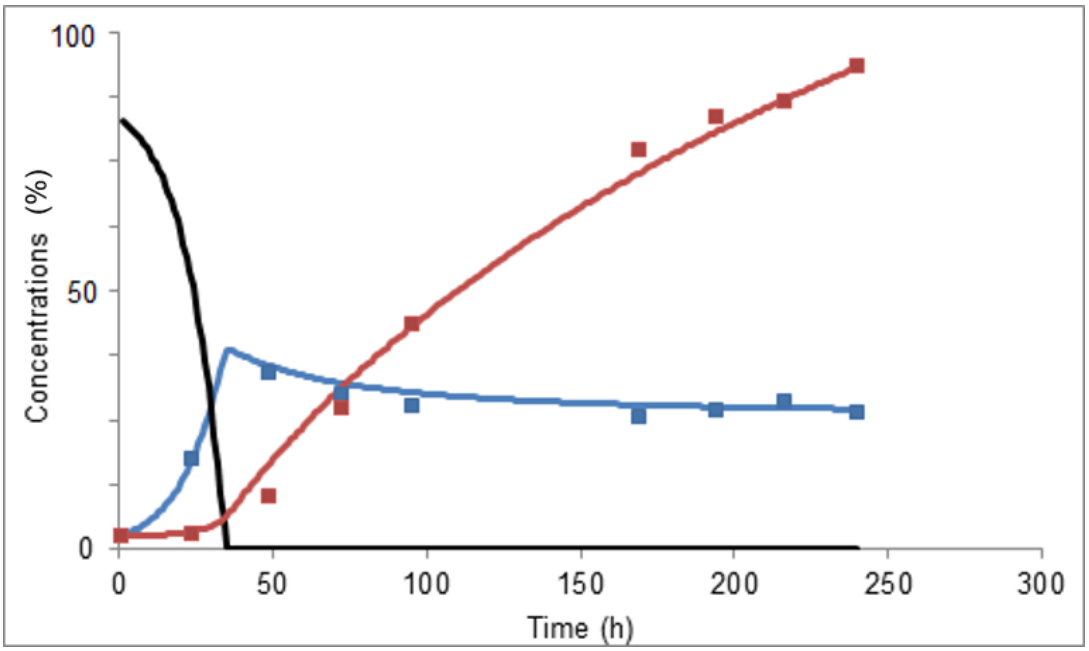

Figure 4.4: Results from the modified model including aging for the culture K1489 (Batch glucose, Fed Batch Lactose at 35 h), in which the marker ■ represents the experimental points of Biomass concentration and the ■ represents the experimental points of Protein concentration. The — represents the model prediction for the biomass concentration, the — represents the model prediction for the proteins concentrations and the — represents the model predictions for the substrate concentration.

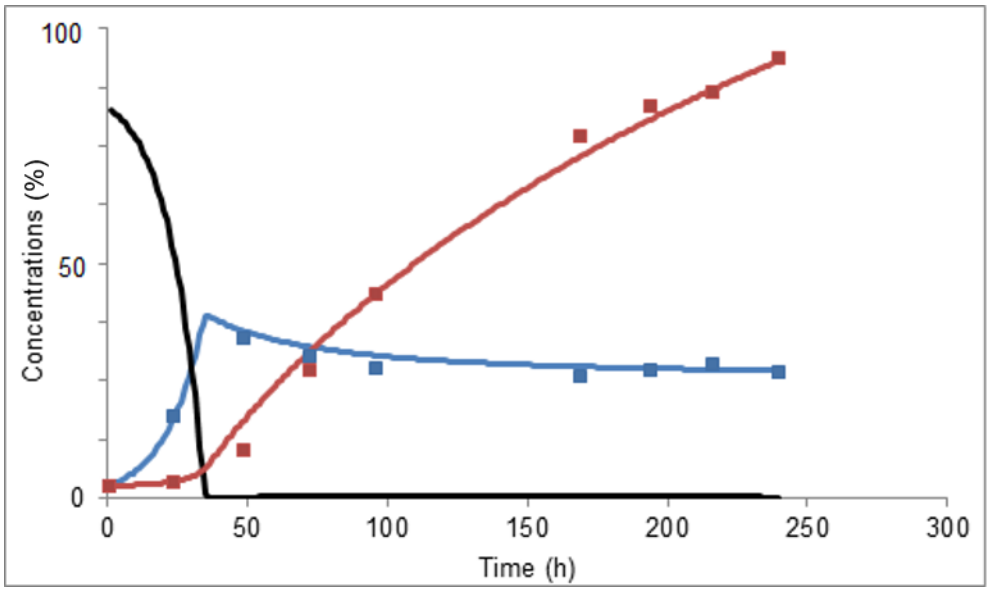

Figure 4.5: Results from the modified model including aging for the culture K1490 (Batch glucose, Fed Batch Lactose at 45 h), in which the marker ■ represents the experimental points of Biomass concentration and the ■ represents the experimental points of Protein concentration. The — represents the model prediction for the biomass concentration, the — represents the model prediction for the proteins concentrations and the — represents the model predictions for the substrate concentration.

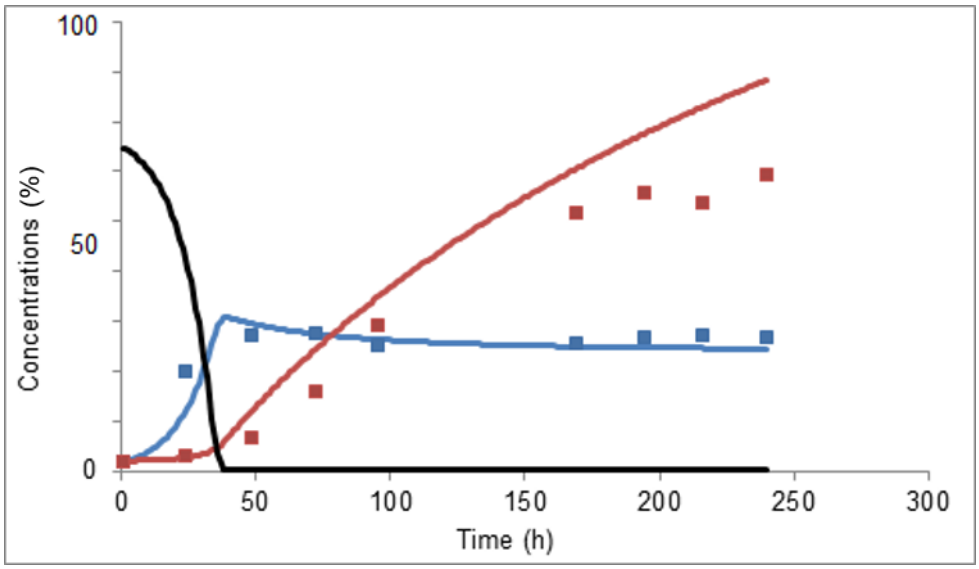

Figure 4.6: Results from the modified model including aging for the culture K1491 (Batch glucose, Fed Batch 75% Glucose 25%Lactose at 35 h), in which the marker ■ represents the experimental points of Biomass concentration and the ■ represents the experimental points of Protein concentration. The — represents the model prediction for the biomass concentration, the — represents the model prediction for the proteins concentrations and the — represents the model predictions for the substrate concentration.

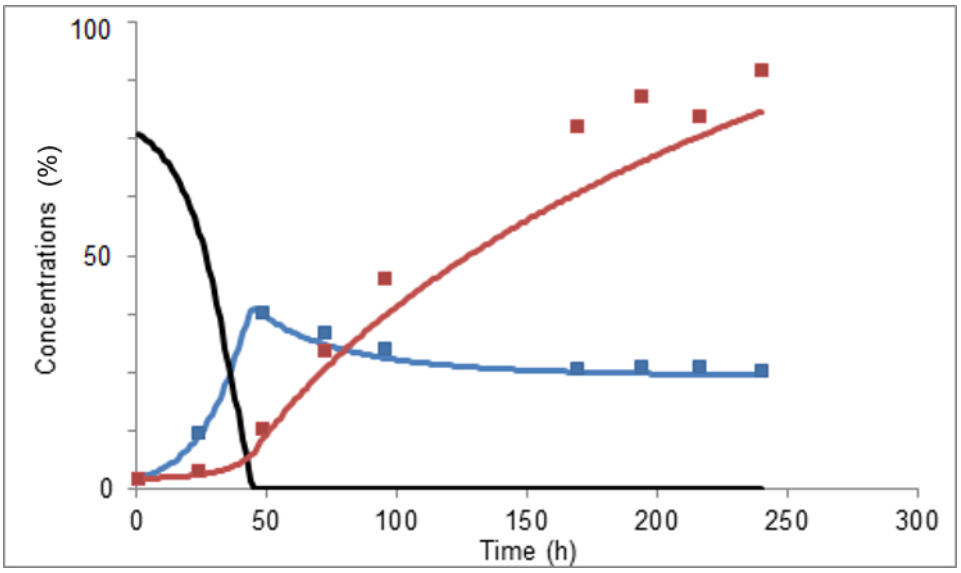

Figure 4.7: Results from the modified model including aging for the culture K1492 (Batch lactose, Fed Batch Lactose at 35 h), in which the marker ■ represents the experimental points of Biomass concentration and the ■ represents the experimental points of Protein concentration. The — represents the model prediction for the biomass concentration, the — represents the model prediction for the proteins concentrations and the — represents the model predictions for the substrate concentration.

From these results it is possible to conclude that the aging mechanism is a good way to improve the modelling of the final points of the fermentations, particularly in what concerns biomass predictions since the model has a good fit for this component for all the cultures. About the protein concentrations prediction the model has a good fit for the first two cultures, an over estimation for the culture K1491 and an under estimation for the K1492.

What is happening by considering a decrease of the value of the q_{pmax}, and consequently, on the q_p is that in the final hours of the fermentation the smaller values of q_p will force the culture to experience a small degree of growth, in order to counterbalance the effect of the lipid consumption mechanism responsible for the loss of biomass, that remains active, keeping the biomass concentration more or less constant as observed.

After this, a relation between the production parameters, q_{pmax} and aging, and the different fed batch compositions in the culture experiments, was sought by changing the values of these variables for each culture but, with no success. This means that the objective from this part of this thesis was not achieved successfully.

Nevertheless, it was verified that by changing the values of the parameters of the mechanism of loss of biomass, k and $Y_{x/p}$, it is possible to obtain better results for the cultures since the model showed a poor fit when using the same values for all the experiments like presented before. In Figure 4.8 a modelling result is presented, for the culture K1492, maintaining the same values for all the kinetic constants presented in Tables 3.2 and 4.3 except for the k and $Y_{x/p}$. The values of these last two parameters that were used in this simulation are presented in Table 4.4.

Table 4.4: Values of the parameters of the new mechanism that were used in the modelling results represented in Figure 4.8.

Parameter	**Value**	**Units**
k	1.5	gX/gP
$Y_{x/p}$	0.8	gX/gP

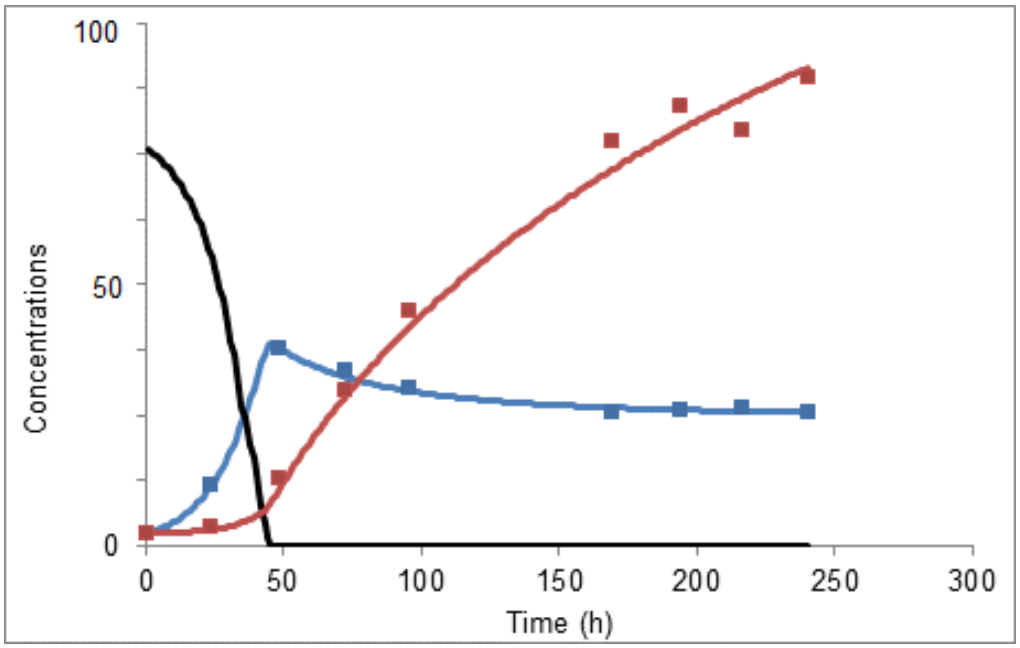

Figure 4.8: Results from the modified model (with Table 4.4 values) including aging for the culture K1492 (Batch Lactose, Fed Batch Lactose at 45 h), in which the marker ■ represents the experimental points of Biomass concentration and the ■ represents the experimental points of Protein concentration. The — represents the model prediction for the biomass concentration, the — represents the model prediction for the proteins concentrations and the — represents the model predictions for the substrate concentration.

The new implementations brought good improvements for the performance of the model and gave new ideas to do further investigations. It is especially important to discover more information about the mechanism of loss of biomass through the consumption of lipid reserves that proved to be a good way to model the experiments. According to the modelling the values of k and $Y_{x/p}$ can change with the different substrates. However it was not possible to stop the mechanism of loss of biomass as it was supposed to, so further work on the model is required to produce a more realistic behaviour. Also, it is proposed that the way the model describes the substrate should be changed. The present model groups all the different sugars as a single substrate and if the sugars were differentiated maybe it would be possible to find a workable relation between the production parameters and the different fed-batch conditions used in the cultures.

4.2 Second Part – Modelling of the Scale up Problems

This part of the thesis has as objective the modelling of experimental cultures under conditions that represent scale-up problems, in order to assess their effect on the production of proteins. Additionally, the aim was to check whether the previously developed model could explain the results or if there was a need to improve it. As presented in the methods, the experiments that were performed to study large-scale reactor mixing problems were the bizone cultures that consist on a system with two reactors, with different sizes, connected to each other. One of the reactors is operated under aerobic conditions and the other under anaerobic conditions. This represents the problem of poor mixing in big bioreactors, with hundreds of cubic meters, that can lead to inefficient dispersion of the bubbles of air and therefore to the creation of zones with low levels of oxygen in the liquid. Also the lactose was only fed to the aerobic reactor which represents the problem of having gradients of nutrient concentration due to its feeding at the top of big bioreactors. Two types of experiments, as mentioned above, will be approached: the

bizone configuration and the inverted bizone configuration. In the first the bigger reactor is the aerobic and the small is the anaerobic. This case represents the situation in which the inefficient mixing induces the formation of small zones that are unaerated. The inverted bizone, as the name suggests, is the case in which the bigger reactor is the anaerobic one representing the possibility of the mixing being so poor that the zones that have low levels of dissolved oxygen represent the majority of the reaction volume. To compare the production results from these experiments Tamiris also did a control run using a one reactor system operated under aerobic conditions with the total volume of liquid equal to that of the 2-reactors system and with the same dissolved oxygen concentration (40%) of saturation.

As in this part the production phase is the relevant one and to simplify computations and the calculations the model simulations only covered the final part os the runs around 160 hours. This was also because the growth pahse was carried out in a single reactor and only 4 days after the beginning of the fed batch phase the system operation with two reactors was started as explained in the methods.

4.2.1 Bizone Experiment Modelling

First in the Figure 4.9 a comparison between the experimental results of the bizone culture K1439 and the control experiment K1452 is presented.

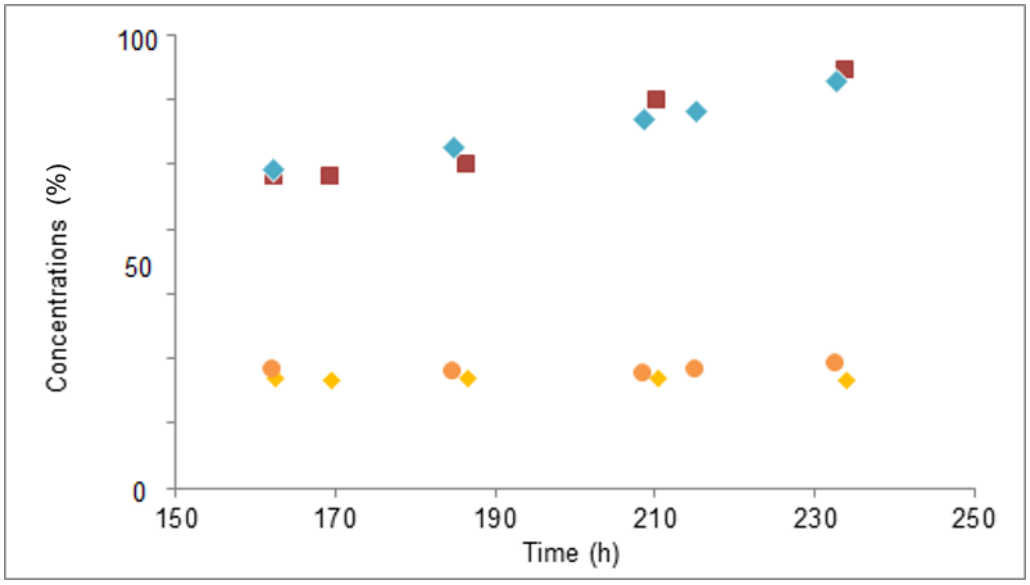

Figure 4.9: Comparison between the experimental results of the experiments bizone K1439 and control K1452. The ◆ represents the biomass concentration from the bizone K1439 and the ● represents the biomass concentration from the control K1452. The ◆ represents the proteins concentration from the control K1452 and the ■ represents the proteins concentration from the bizone experiment.

As it can be seen in Figure 4.9 there is no loss of production between the control and the bizone experiments, which means that the q_p that was measured in the laboratory is the same for both experiments. The values of the experimental q_p are presented below in Table 4.5. What this results says is that the anaerobic reactor is not big enough to affect the global production capacity of the system since in this reactor there is no biological activity due to the fact that the dissolved oxygen concentration is close to zero.

Table 4.5: Measured values of q_p from the experiments K1439 (bizone) and K1452 (control).

Parameter	Value	Units
q_p^* exp. control	72	%
q_p^* exp. bizone	72	%

It was then checked whether the initial model could predict the same results for both experiments. In Figure 4.10 the modelling results for both runs, bizone and control, are presented. The parameters used in this modelling are those presented in Table 3.2 and in Table 4.6 below.

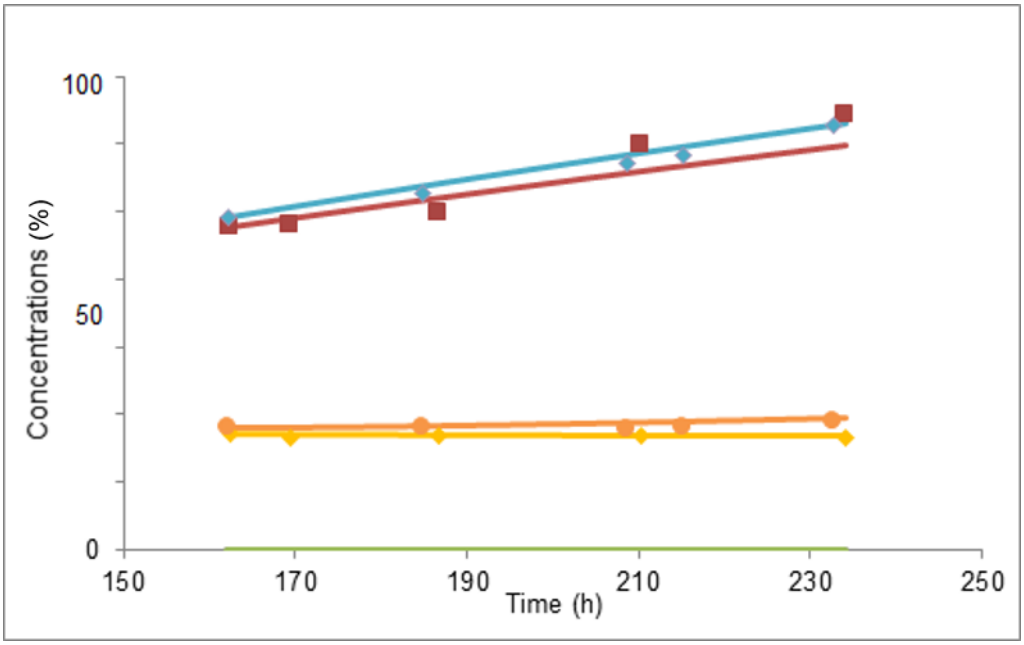

Figure 4.10: Modelling results of the cultures K1439 (bizone) and K1452(control). The markers have the same legend as Figure 4.9. The — represents the model predictions of biomass concentrations from the bizone culture. The — represents the model predictions of biomass concentrations from the control culture. The — represents the model predictions of protein concentrations from the bizone culture. The — represents the model predictions of proteins concentrations from the control culture. The — represents the model predictions of substrate concentrations from the bizone culture. The — represents the model predictions of substrate concentrations from the control culture.

Table 4.6: Values of the Kinetic Parameters that were used to obtain the modelling results in this part of the thesis (chapter4.2).

Parameter	Value	Units
μ_{max} (K1439)	0.08	h^{-1}
μ_{max} (K1452)	0.08	h^{-1}
q_{pmax}^* (K1439)	88	%
q_{pmax}^* (K1452)	88	%

From the analysis of the results shown in Figure 4.10 it can be seen that the model provides a good prediction of the behaviour of the control experiment giving the same value for the q_p that was measured experimentally. For the bizone experiment the model gives a good prediction for the biomass and protein concentrations even though, the proteins curve is not adjusted to the experimental points giving a q_p value that is slightly smaller when compared with the experimental measurement (64%). However, the

difference of q_p value obtain from the model of the bizone when compared with the experimental value is not significant since it is within the experimental error reported for the measures that were carried out in the laboratory.

Besides run K1439, Tamiris did also other bizone experiments as repetitions of K1439. The modelling of the repetitions was done successfully with the same values of the parameters, giving the same values of q_p that were found experimentally, and these results can be found in Appendix B.

It should however be noted that it was necessary to introduce a modification in the model regarding the maintenance coefficients. In the first attempts at modelling the bizone experiment the predicted values of dissolved oxygen concentration of the anaerobic reactor became negative after a certain time. This happened because the values of q_{O_2} were too high due to the maintenance term since there was almost no oxygen consumption sources given that the terms of growth and protein production were small. To solve this problem, it was decided to introduce the variation of the maintenance coefficient for the consumption of substrate according to a Monod type equation for the substrate and a Michaelis-Menten term for the oxygen as presented below in Equation A.18. This mean that as the oxygen available decreases so does the amount of substrate that can be metabolized for maintenance and so the values of q_{O_2} decrease allowing the dissolved oxygen concentration to values remain positive.

$$m_{\text{s}} = m_{\text{s max}} \frac{[S]}{K_{\text{s M}} + [S]} \times \frac{[O_2]}{K_{\text{O}_2\text{ M}} + [O_2]} \tag{4.6}$$

The $m_{s\ max}$ represents the maximum value that the maintenance coefficient can reach, the $K_{s\ M}$ is the Monod constant for the substrate for maintenance and the $K_{O_2\ M}$ is the Michaelis-Menten term for the oxygen for maintenance. The values of these new kinetic constants that best fit the experimental points are presented below in Table 4.7.

Table 4.7: Values of the parameters that define the new maintenance coefficient variantion assumption.

Parameter	Value	Units
$m_{s\ max}$	0.01	gS/gX/h
$K_{s\ M}$	0.001	gS/L
$K_{O_2\ M}$	0.0001	gO_2/L

4.2.2 Inverted Bizone Experiment Modelling

After checking that the model had a good prediction performance for the bizone experiments and after finding the correct kinetic constant values it was further tested on the inverted bizone experimental results. First, in Figure 4.11 a comparison between the experimental results of the control run K1452 and the inverted bizone K1455 is presented.

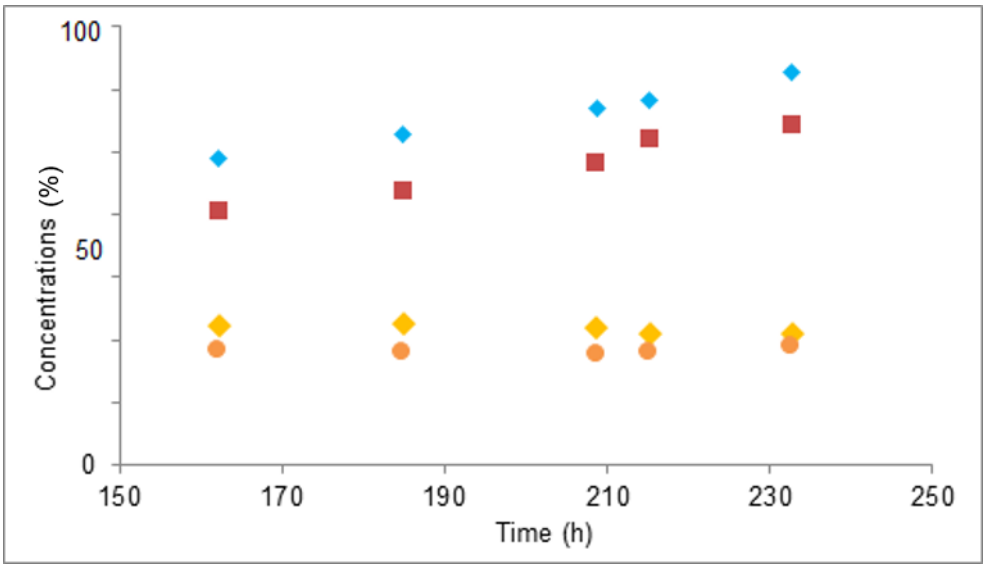

Figure 4.11: Comparison between the experimental results of the experiments inverted bizone K1455 and control K1452. The ◆ represents the biomass concentration from the inverted bizone experiment and the ● represents the biomass concentration from the control experiment K1452. The ◆ represents the proteins concentration from the control experiment K1452 and the ■ represents the proteins concentration from the bizone experiment.

As it can be seen in Figure 4.11 there is a decrease in q_p from the inverted bizone when compared with the control value that was measured experimentally. This means that the loss of biological activity in the system, due to the fact that the bigger reactor is anaerobic, is not negligible. However, there is still some protein production though smaller than in the control reactor. In Table 4.8 the value of q_p obtained experimentally for the inverted bizone experiment is presented.

Table 4.8: Experimentally measured value of q_p for the inverted bizone run.

Parameter	Value	Units
q_p^* exp. inverted bizone	44	%

The subsequent modeling objective was to see once again if the model can explain this reduction in q_p that was verified in the laboratory or if is it necessary to improve the model in order to obtain a good prediction of the results. In Figure 4.12 the first attempt at modelling the inverted bizone is presented. All modelling attempts were done using the same kinetic parameters that were used in the bizone modelling.

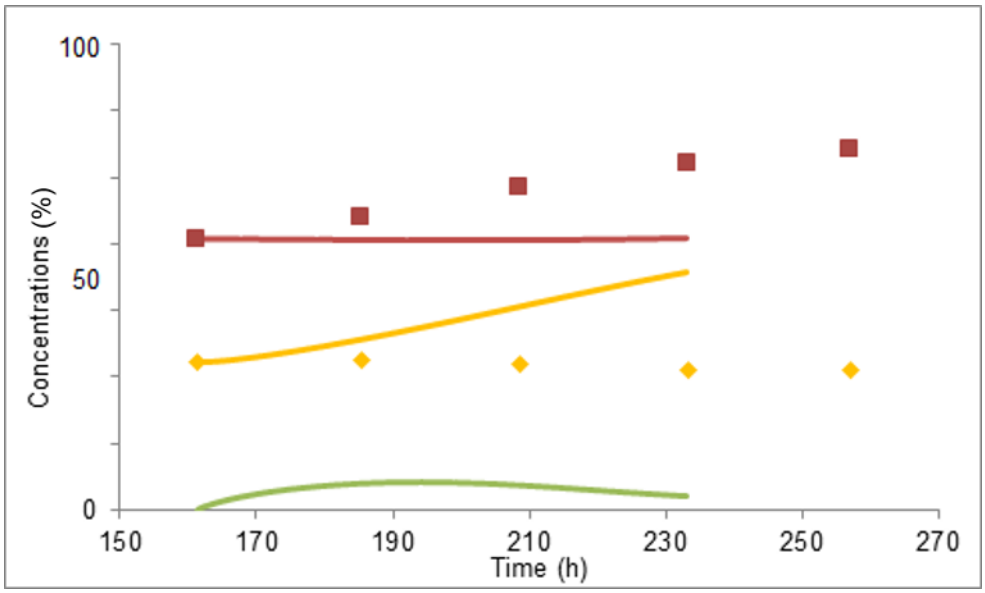

Figure 4.12: Modelling results for the culture K1455 (inverted bizone) in which the marker ◆ represents the experimental points of biomass concentration and the ■ represents the experimental points of protein concentration. The — represents the model prediction for biomass concentration, the — represents the model prediction for protein concentration and the — represents the model predictions for the substrate concentration.

By analysing Figure 4.12 it can be clearly understood that the model does not predict at all the behaviour of the inverted bizone culture. The results of the model are to be expected taking into account its features. As there is a big part of the volume of the system that is unaerated the sugar substrate starts to accumulate in this zone because as there is no oxygen there is no biomass or protein production, therefore the substrate is not consumed. Above a certain value of substrate concentration, the fungal biomass starts to grow in the aerobic reactor instead of producing cellulases. However, like explained before, this is not what happened experimentally, so some thought was required on what features could be implemented in the model in order for it to predict the behaviour of the inverted bizone culture. Like it was said before in the laboratory it was observed that even when protein production suffered a loss there is still some biological activity apparently also in the anaerobic zone, which the model does not predict. This can only mean that experimentally, there is some protein production in the anaerobic reactor and, in order for it to occur there must exist some kind of transport mechanism of oxygen from the aerobic reactor to the anaerobic reactor that it is not being taken into account by the model. Notice that some dissolved oxygen transfer is already being taken into consideration in the liquid recirculation between the reactors but as it can be seen in Figure 4.12 is not enough to explain the experimental results.

At this point some thought was given to phenomena that could explain the additional transport of oxygen to the anaerobic reactor and two possible theories came up:

1. Recirculation of bubbles of air (gas hold-up) together with the broth;
2. Oxygen can be stored and transported inside the fungal cells.

During the course of the experiment it was seen that there were some bubbles of gas that were transported between the two reactors but its flow rate was not known. To include this phenomenon in the model it was necessary to include some terms in the equations that define the gas phase of each reactor. The new equations for the gas phase for one of the reactors (as an example), considering the

recirculation of gas bubbles are presented below:

$$\frac{d[O_2]_{\text{gas R1}}}{dt} = \frac{(Q_{O_2\,\text{in R1}} - Q_{O_2\,\text{out R1}} - OTR_{\text{R1}} \times V_{\text{L R1}})}{V_{\text{gas R1}}} + \frac{(Qrg_{\text{2-1}} \times f_{O_2\,\text{R2}} - Qrg_{\text{1-2}} \times f_{O_2\,\text{R1}}) \times 32}{V_{\text{gas R1}}} \quad (4.7)$$

$$f_{O_2\,\text{R1}} = \frac{[O_2]_{\text{gas}}}{32} \times \frac{RT}{P} \times 1000 \quad (4.8)$$

$$OTR_{\text{R1}} = k_l a_{\text{R1}} (K_{\text{H}} \times f_{O_2\,\text{R1}} \times P \times 32 - [O_2]_{\text{R1}}) \quad (4.9)$$

$$Q_{N_2\,\text{out R1}} = Q_{N_2\,\text{in R1}} + (Qrg_{\text{2-1}} \times (1 - f_{O_2\,\text{R2}}) - Qrg_{\text{1-2}} \times (1 - f_{O_2\,\text{R1}})) \times 28 \quad (4.10)$$

$$Q_{O_2\,\text{out R1}} = \frac{Q_{N_2\,\text{out R1}}}{28} \frac{1 - f_{O_2}}{f_{O_2}} \times 32 \quad (4.11)$$

As the gas flow rate in the recirculation loop was not known, some tests were carried out with arbitrary values in an attempt to find the value of gas hold-up inside the recirculation lines that could explain the biomass and protein concentration results. The value for the gas hold-up in the recirculation that was found to lead to a good prediction of the results was 40%. In Figure 4.13 are presented the modelling results of the inverted bizone experiment with 40% of gas hold-up in the recirculation lines.

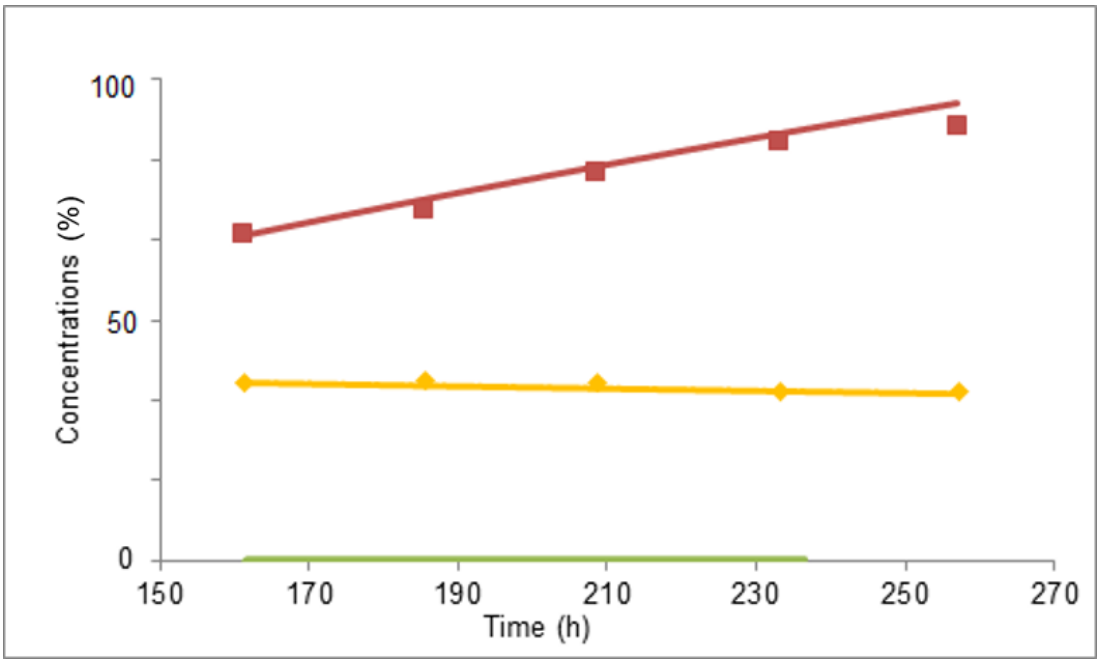

Figure 4.13: Modelling results for the culture K1455 (inverted bizone), considering 40% gas hold-up in the recirculation lines, in which the marker ◆ represents the experimental points of biomass concentration and the ■ represents the experimental points of protein concentration. The — represents the model prediction for the biomass concentration, the — represents the model prediction for the protein concentration and the — represents the model predictions for the substrate concentration.

From the results presented in Figure 4.13 it can be said that the recirculation of gas can be one explanation for the experimental results of the inverted bizone culture since the model shows a good fit to the experimental points. However, in order to produce these results it was necessary to consider a gas hold-up of 40% inside the recirculation lines which probably is not realistic because this value is too

big.

To check on this idea, Tamiris repeated the experiment in the lab during which she measured the gas flow rate in the recirculation lines between the reactors and found that the real gas hold-up is around 17%. Setting the hold-up at this new value the modelling of the inverted bizone was repeated and the result can be found below in Figure 4.14.

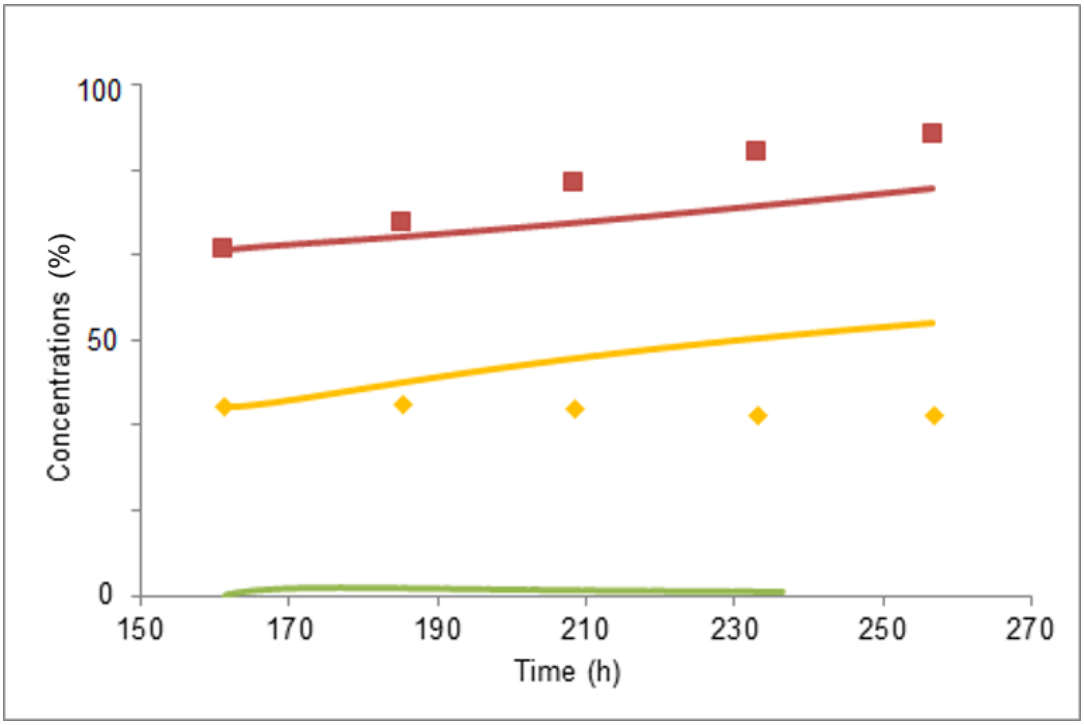

Figure 4.14: Modelling results for the culture K1455 (inverted bizone), considering 17% gas hold-up in the recirculation lines, in which the marker ◆ represents the experimental points of biomass concentration and the ■ represents the experimental points of protein concentration. The — represents the model prediction for the biomass concentration, the — represents the model prediction for the protein concentration and the — represents the model predictions for the substrate concentration.

By analysing Figure 4.14 it can be understood that using the model with recirculation of gas at 17% of hold-up is not enough to explain the experimental results of the inverted bizone. However, by comparing these results with those presented in Figure 4.11 we can see that using 17% of hold-up the model can explain part of the results predicting some protein and biomass production and consequently less substrate accumulation.

Nonetheless, the recirculation of gas by itself is not enough to improve the quality of the model predictions to the desired level, therefore the second option was considered that consists in the cells being able to store oxygen to be used in the anaerobic zone. This theory can be substantiated by assuming that when the fungus cells are in the aerobic reactor they take up oxygen from the liquid which is transformed into an intermediary molecule that functions as an oxidative power transporter. This intermediary (identified as W) can be accumulated inside the cells up to a maximum value that defines the storage capacity of the cells for this molecule and can be used in the metabolism of the cells replacing the oxygen. The reaction of transforming the oxygen into W was modelled as a first order on the oxygen concentration.

To implement this theory, we had to change the structure of the model by creating a new component, the intermediary molecule that we called W, and define the maximum amount of W that the cells can store that we called W_{max}. First we defined the W_{max} concentration as proportional to the biomass

concentration through Equation 4.12:

$$[W_{\text{max}}] = A[X] \tag{4.12}$$

Then a mass balance to W was required. This balance is presented below in Equation 4.13:

$$\frac{d[W]}{dt} = K_{\text{W}}[O_2]([W_{\text{max}}] - [W]) - q_{\text{W}}[X] \tag{4.13}$$

The first term defines the amount of W that can be formed and stored inside the cells and the second term is the amount of W that is consumed by the biomass to grow, produce cellulases and for maintenance. The K_W represents the rate of the transport and transformation of oxygen into W. The q_W represents the specific consumption rate of W that now replaces q_{O_2} in the model.

The idea with this theory is that when the cells are in the aerobic reactor they store W at a concentration close to the value for W_{max} and even as they consume it the storage level remains close to the maximum value. When the cells arrive at the anaerobic reactor they start to consume the stored W but now as the oxygen levels are very low the W is not replenished as fast as it is consumed and the W concentration drops to low values (the W_{max} value is around 0.05 gW/L). As the cells arrive back in the aerobic reactor they refill the W storage again.

All equations that define the model were also modified by replacing the oxygen concentration and the Michaelis-Menten constants and the yields related with oxygen by the W concentration and the constants related with W. The new equations of the model are presented below:

$$\mu = \frac{\mu_{\text{max}} \times [S]}{K_{\text{s}\mu} + [S]} \times \frac{[W]}{K_{\text{W}\mu} + [W]} \tag{4.14}$$

$$q_{\text{p}} = (\frac{q_{\text{pmax}} - q_{\text{pmin}}}{1 + [X]/K_{\text{iXP}}} + q_{\text{pmin}}) \times \frac{[S]}{K_{\text{SP}} + [S]} \times \frac{[W]}{K_{\text{WP}} + [W]} \times \frac{K_{\text{iXP}}}{K_{\text{iXP}} + [S]} \tag{4.15}$$

$$q_{\text{w}} = \frac{\mu}{Y_{\text{x/W}}} + \frac{q_{\text{p}}}{Y_{\text{p/W}}} + Y_{\text{W/s}}{}^{\text{m}} \times m_{\text{s}} \tag{4.16}$$

$$m_{\text{s}} = m_{\text{s max}} \frac{[S]}{K_{\text{s M}} + [S]} \times \frac{[W]}{[W] + K_{\text{W M}}} \tag{4.17}$$

The values of the Michaelis-Menten constants and the yields related with W were kept those that were presented in the Table 3.2 since it was considered that 1 gram of oxygen is equivalent to 1 gram of W.

The mass balance to the dissolved oxygen was also changed because now the decrease of oxygen concentration in the medium is not due to its direct consumption but due to the amount of oxygen that is transferred to this reservoir inside the cells. The new mass balance to the oxygen in the liquid phase is presented below by Equation 4.18:

$$\frac{d[O_2]}{dt} = \frac{-K_{\text{W}}[O_2]([W_{\text{max}}] - [W])}{Y_{\text{W/O}_2}} + k_{\text{l}}a([O_2]^{\star} - [O_2]) - \frac{[O_2]}{V_{\text{L}}}\Delta Q_{\text{v}} \tag{4.18}$$

The Y_{W/O_2} is the yield of the transformation of oxygen to W that was assumed to be 1 in mass units, as stated above.

After these implementations, some attempts at modelling the inverted bizone were made in order to find the correct values for the variables that define this new mechanism of storage of oxygen. The optimal values that were found for the new parameters are presented in Table 4.9.

Table 4.9: Values of the kinetic parameters specific for the oxygen storage theory.

Parameter	Value	Units
K_w	195	gW/gO_2
A	0.0528	gW/gX

With the right values for the new kinetic parameters it was possible to model the inverted bizone experimental results. In Figure 4.15 are presented the modelling results for the inverted bizone run considering the storage of oxygen inside the cells.

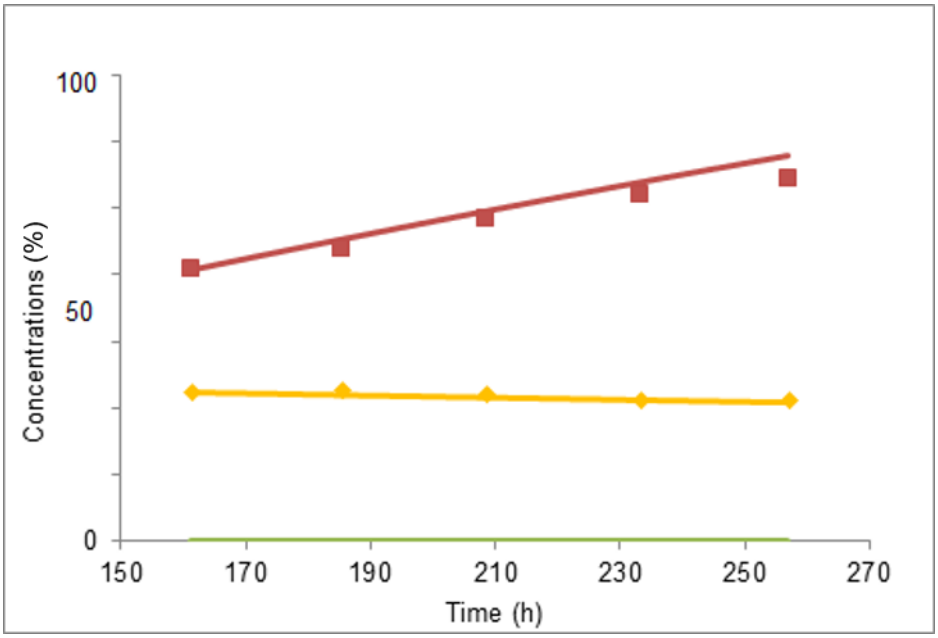

Figure 4.15: Modelling results for culture K1455 (inverted bizone), considering the storage of oxygen inside the cells, in which the marker ◆ represents the experimental points of biomass concentration and the ■ represents the experimental points of protein concentration. The — represents the model prediction for the biomass concentration, the — represents the model prediction for the protein concentration and the — represents the model predictions for the substrate concentration.

In Figure 4.15 it can be seen that this theory works very well since the model gives a good prediction of the experimental results. In Table 4.10 the value of q_p obtained by the model with the W kinetics is presented.

Table 4.10: Value of q_p predicted by the model with the W kinetics.

Parameter	Value	Units
q_p^* model inverted bizone	48	%

The q_p value predicted by the model is practically the same as that obtained experimentally (deviation of 9%) which means that the model gives a good prediction of the experimental results. However, this is just a theory that might not be what really happens. Furthermore, no specific bibliographic information was found about the possibility of storage oxygen by any filamentous fungus. This is just an apparent kinetics possibility to try to explain the experimental results. Experimentally this process of storage of oxidative power is probably much more complex than the way we chose to model it but as it was explained before in the first part of the results of this thesis, the objective is to keep the model as simple as possible.

To validate this new kinetic hypothesis, the bizone and the control experiments were also modelled using the same structure and values of the parameters that were employed in the modelling of the inverted bizone. The results obtained with the new kinetics were exactly the same that were reached with the standard oxygen consumption kinetics, which is an indication of the potential usefulness of the new kinetics.

However, it was already shown that there was recirculation of gas bubbles between the two reactors with 17% hold-up in the liquid stream that could be responsible for a part of the productivity of the culture as it was seen in Figure 4.14. In this way, we thought that probably the more realistic approach is to consider the two phenomena at the same time: the bubble recirculation and the intracellular storage of oxygen. So a modelling test was done considering the 17% of hold-up and the W kinetics. However, the value of A was changed (0.002 gW/gX) in order to give a lower value of W_{max}, around 0.02 gW/L, since in this case there is no need to use such a large value of W because there is also the oxygen that is transported in the bubbles of air in the recirculation. In Figure 4.16 the result of the modelling of the inverted bizone considering the two phenomena is presented.

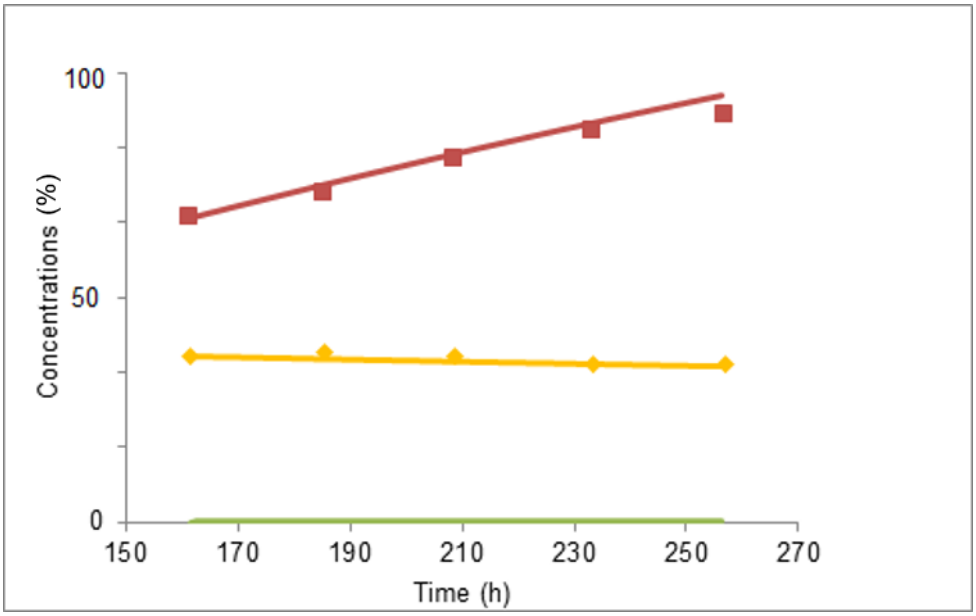

Figure 4.16: Modelling results for the culture K1455 (inverted bizone), considering 17% of gas hold-up in the recirculation stream and the W kinetics, in which the marker ◆ represents the experimental points of biomass concentration and the ■ represents the experimental points of protein concentration. The — represents the model prediction for the biomass concentration, the — represents the model prediction for the protein concentration and the — represents the model predictions for the substrate concentration.

From Figure 4.16 it can be seen that the combination of the two phenomena gives a good explanation of the experimental results with the same q_p value that was obtained by the model which considered the W kinetics alone.

4.2.3 Verification of the complete mixing assumption

When the W theory was inserted in the model it was assumed that the medium was perfectly mixed which means that all the cells have the same residence time in the aerated reactor and therefore the same amount of W. However, what really happens is that the different cells in the fungus population can have different residence times in each reactor which influences directly the amount of W that they have been able to store and consequently the overall protein and biomass production.

To check if the assumption of a perfectly mixed system is very far from reality some calculations in an excel sheet were made, considering only one reactor in anaerobic conditions, for two different cases.

The first case is to consider an anaerobic CSTR with the same conditions used in the laboratory (volume and liquid flow rate) a perfectly mixed medium and certain biomass and substrate concentrations that enter the reactor with an initial concentration of Wi as presented in Figure 4.17.

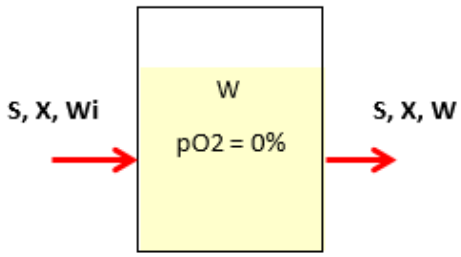

Figure 4.17: Representation of the system considered for the verification of the assumption of a perfectly mixed system.

Then a mass balance to W was done to calculate its the concentration at the outlet of the reactor as presented in Equation 4.19:

$$\frac{d[W]}{dt} = -q_W[X]V_L + Q_{in}[Wi] - Q_{out}[W] \tag{4.19}$$

As the system is admitted to be at steady state d[W]/dt=0 and the Q_{in}=Q_{out}. By solving this equation the outlet concentration of W was found and with this value the value of q_W was calculated. The objective now is to find the value of q_W but considering the residence time distribution (RTD) of a CSTR and compare the value with that obtained in the first case that was just presented.

So for the second case the same system with the same conditions was considered. First, the values of concentration of W in the culture were calculated for all the residence times from 0 to 17 minutes which is the residence time in the reactor admitted for the first case. The distribution of the obtained values of W concentration is represented below in Figure 4.18.

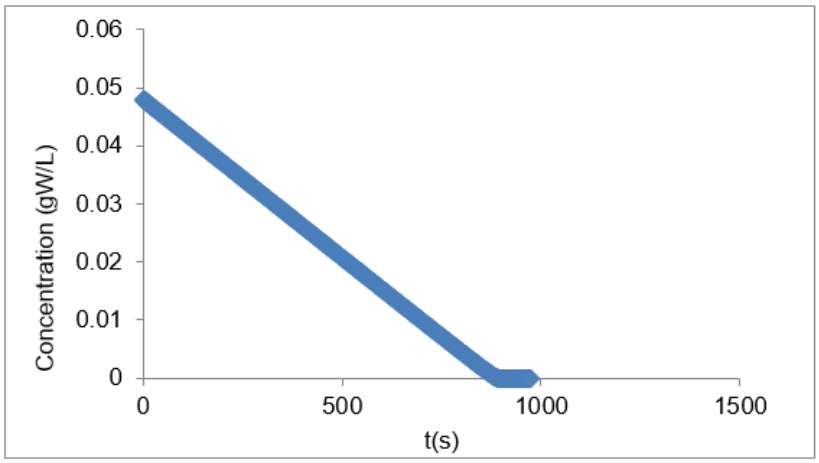

Figure 4.18: Representation of the distribution of values of concentration of W, as a function of the residence time in the anaerobic reactor.

So what happens is that the biomass population enters the reactor with a concentration of W close to the maximum value and as the residence time increases the W is consumed further and for the population fraction that stays in the reactor up to the mean residence time (17 minutes) the W concentration

becomes is close to zero.

Then the q_W value for the different residence times was also calculated and its distribution is represented in Figure 4.19 below:

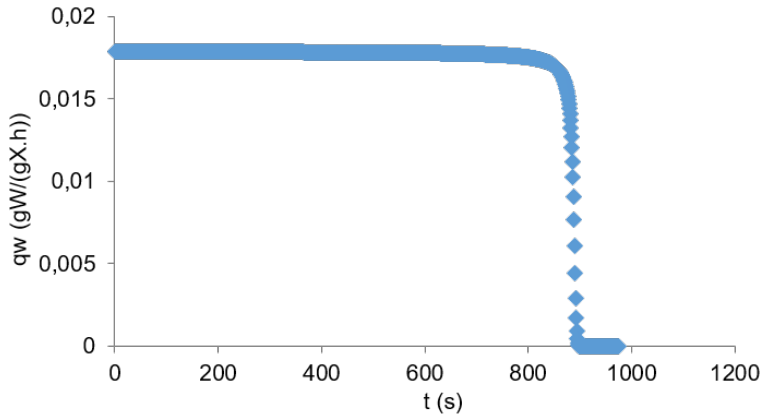

Figure 4.19: Representation of the distribution of q_W values for different residence times of the biomass in the anaerobic reactor.

Then the average value of the q_W was calculated for each residence time value (t) through the integral presented below in the Equation 4.20.

$$\bar{q_W}(t) = \frac{1}{t}\int_0^t q_W(\theta)d\theta \tag{4.20}$$

Then the global average value for q_W of all elements of the culture taking into account the ideal form of the RTD was calculated by Equation 4.21.

$$\bar{\bar{q_W}} = \int_0^\infty \frac{1}{\theta}e^{-t/\theta}q_W(t)dt \tag{4.21}$$

The values of the q_W calculated for both cases are presented below in the Table 4.11.

Table 4.11: Values of q_W obtained for both cases with a residence time of 17 min.

Parameter	Value	Units
q_w perfect mixture	0.0155	gW/(gX.h)
q_w RTD	0.015	gW/(gX.h)

The deviation between the values is equal to 3% which means that the assumption of a perfectly mixed system does not introduce a great error in the results of the model for the conditions that were used in the laboratory.

Then the same calculations were made for both cases but now with different conditions, considering an average residence time of 34 min, the double of the value used before. The values of q_W obtained are presented below in the Table 4.12.

Table 4.12: Values of q_W obtained for both cases with a residence time of 34 min.

Parameter	Value	Units
q_w perfect mixture	0.012	gW/(gX.h)
q_w RTD	0.008	gW/(gX.h)

Now with this conditions there is a big difference between the values of specific consumption of W which means that if we want to use the model to simulate other experiments with different conditions we have to take into account the RTD in the calculations.

Chapter 5

Conclusions

From the first part of the results it can be concluded that the lipid consumption mechanism of loss of biomass provides a good explanation of the behaviour of the culture during the transition between the batch and fed-batch culture stages. In order to have a better fit of the experimental points to the model it is however required to consider an aging effect on the culture. However, it was not possible to find an explanation for the differences between the four modelled cultures since we could not estabilsh a rationale for changing the production parameters for each culture. Additional studies are required to validate the proposed mechanisms. Furthermore, in order for the model to better describe culture behaviour under different fed batch compositions it is proposed that the different sugars that are involved in the process should be differentiated considering their effect on the growth of the biomass and production of cellulases.

Regarding the second part of the results, the initial model is good enough to explain the results of the bizone experiment but overestimates the effect of large heterogeneities that are expressed by the experimental results of the inverted bizone experiment. To improve the model two different phenomena were considered: air bubbles transported in the recirculation liquid and the storage of oxygen inside the cells. The first only explains part of the deviation between the initial model and the experimental results. The storage of oxygen was indicated to be a possible explanation for the production results of all the experimental runs (single reactor, bizone and inverted bizone). A combination of both phenomena seems to be the most realistic approach among those tested giving a good prediction of the experimental results of the inverted bizone experience.

The assumption of a perfectly mixed system in the conditions that were used in the laboratory was proven not to introduce a major error in the results given by the model for the conditions used in the lab experiments, namely the average retention time in the anaerobic section of the bizone system. However, it was found that if other conditions are used the RTD has to be taken into account in the calculations in order to avoid a big deviation between the model predictions and the experimental results.

Bibliography

Abu-Ghannam, Nissreen; Balboa, Elena (2018): Biotechnological, food, and health care applications. : Sustainable Recovery and Reutilization of Cereal Processing By-Products: Elsevier, pp. 253–278.

Ahamed, Aftab; Vermette, Patrick (2009): Effect of culture medium composition on *Trichoderma reesei*'s morphology and cellulase production. Bioresource Technology 100 (23), pp. 5979–5987. DOI: 10.1016/j.biortech.2009.02.070.

Alam, Firoz; Mobin, Saleh; Chowdhury, Harun (2015): Third Generation Biofuel from Algae. Procedia Engineering 105, pp. 763–768. DOI: 10.1016/j.proeng.2015.05.068. Arora, Richa; Sharma, Nilesh K.; Kumar, Sachin; Sani, Rajesh K. (2019):

Lignocellulosic Ethanol. Feedstocks and Bioprocessing. In : Bioethanol Production from Food Crops: Elsevier, pp. 165–185.

Bader, J.; Klingspohn, U.; Bellgardt, K.-H.; Schügerl, K. (1993): Modelling and simulation of the growth and enzyme production of *Trichoderma reesei* Rut C30. Journal of Biotechnology 29 (1-2), pp. 121–135. DOI: 10.1016/0168-1656(93)90045-O.

Bannari, Rachid; Bannari, Abdelfettah; Vermette, Patrick; Proulx, Pierre (2012): A model for cellulase production from *Trichoderma reesei* in an airlift reactor. Biotechnol. Bioeng. 109 (8), pp. 2025–2038. DOI: 10.1002/bit.24473.

Bertrand, Emmanuel; Vandenberghe, Luciana P. S.; Soccol Carlos R.; Sigoillot, Jean-Claude, Faulds Craig (2011): First Generation Bioethanol. Carlos Ricardo Soccol, Satinder Kaur Brar, Craig Faulds, Luiz Pereira Ramos (Eds.): Green Fuels Technology. Biofuels: Springer, pp. 175–212.

Bischof, Robert H.; Ramoni, Jonas; Seiboth, Bernhard (2016): Cellulases and beyond. The first 70 years of the enzyme producer *Trichoderma reesei*. Microb Cell Fact 15 (1), p. 24. DOI: 10.1186/s12934-016-0507-6.

Cappello, Vincenzo; Plais, Cécile; Vial, Christophe; Augier, Frédéric (2020): Bubble size and liquid-side mass transfer coefficient measurements in aerated stirred tank reactors with non-Newtonian liquids. Chemical Engineering Science 211. DOI: 10.1016/j.ces.2019.115280.

Cardona, C. A.; Quintero, J. A.; Paz, I. C. (2010): Production of bioethanol from sugarcane bagasse. Status and perspectives. Bioresource Technology 101 (13), pp. 4754–4766. DOI: 10.1016/j.biortech.2009.10.097.

Chaudhuri, B. K.; Sahai, Vikram (1993): Production of cellulase using a mutant strain of *Trichoderma reesei* growing on lactose in batch culture. Appl Microbiol Biotechnol 39 (2). DOI: 10.1007/BF00228605.r Chaudhuri, B. K.; Sahai, Vikram (1994): Comparison of growth and maintenance parameters for cellulase biosynthesis by *Trichoderma reesei*-C5 with some published data. Enzyme and Microbial Technology 16 (12), pp. 1079–1083. DOI: 10.1016/0141-0229(94)90146-5.

Chen, Hongzhang (2014): Biotechnology of lignocellulose. Theory and practice / Hongzhang Chen. Dordrecht: Springer.

Chengcheng Li; Ai-Ping Pang; Hang Yang; Roujing Lv; Zhihua Zhou; Fu-Gen Wu; Fengming Lin

(2019): Tracking localization and secretion of cellulase spatiotemporally and directly in living *Trichoderma reesei*. Biotechnol Biofuels 12 (1), pp. 1–12. DOI: 10.1186/s13068-019-1538-0.

Cherubini, Francesco; Strømman, Anders H. (2011): Principles of Biorefining. In : Biofuels: Elsevier, pp. 3–24.

Dahman, Yaser; Dignan, Cherilyn; Fiayaz, Asma; Chaudhry, Ahmad (2019): An introduction to biofuels, foods, livestock, and the environment. In : Biomass, Biopolymer-Based Materials, and Bioenergy: Elsevier, pp. 241–276.

Darabzadeh, Nazanin; Hamidi-Esfahani, Zohreh; Hejazi, Parisa (2019): Optimization of cellulase production under solid-state fermentation by a new mutant strain of *Trichoderma reesei*. Food science & nutrition 7 (2), pp. 572–578. DOI: 10.1002/fsn3.852.

Dias, Marina O.S.; Junqueira, Tassia L.; Rossell, Carlos Eduardo V.; Maciel Filho, Rubens; Bonomi, Antonio (2013): Evaluation of process configurations for second generation integrated with first generation bioethanol production from sugarcane. Fuel Processing Technology 109, pp. 84–89. DOI: 10.1016/j.fuproc.2012.09.041.

Doriya, K.; Jose, N.; Gowda, M.; Kumar, D. S. (2016): Solid-State Fermentation vs Submerged Fermentation for the Production of l-Asparaginase. Se-Kwon Kim (Ed.): Marine enzymes biotechnology. Production and industrial applications. Part I, Production of enzymes / edited by Se-Kwon Kim, vol. 78. Amsterdam: Academic Press (Advances in Food and Nutrition Research, 78), pp. 115–135.

Druzhinina, Irina S.; Kubicek, Christian P. (2017): Genetic engineering of *Trichoderma reesei* cellulases and their production. Microbial biotechnology 10 (6), pp. 1485–1499. DOI: 10.1111/1751-7915.12726.

Etxebeste, Oier; Espeso, Eduardo A. (2016): Neurons show the path. Tip-to-nucleus communication in filamentous fungal development and pathogenesis. FEMS microbiology reviews 40 (5), pp. 610–624. DOI: 10.1093/femsre/fuw021.

Fan, Liangliang; Zhang, Yaning; Liu, Shiyu; Zhou, Nan; Chen, Paul; Cheng, Yanling et al. (2017): Bio-oil from fast pyrolysis of lignin. Effects of process and upgrading parameters. Bioresource Technology 241, pp. 1118–1126. DOI: 10.1016/j.biortech.2017.05.129.

Gabelle, J.-C. (2012a): Local and global analysis of the hydrodynamics and the transfer of matter in fluids with complex rheology, characteristic of fermentation media. Doctoral thesis. IFPEN.

Gabelle, J.-C.; Jourdier, E.; Licht, R. B.; Ben Chaabane, F.; Henaut, I.; Morchain, J.; Augier, F. (2012b): Impact of rheology on the mass transfer coefficient during the growth phase of *Trichoderma reesei* in stirred bioreactors. Chemical Engineering Science 75, pp. 408–417. DOI: 10.1016/j.ces.2012.03.053.

Gavrilescu, Maria (2014): Biorefinery Systems. In : Bioenergy Research: Advances and Applications: Elsevier, pp. 219–241.

Geng, Anli (2014): Genetic Transformation and Engineering of *Trichoderma reesei* for Enhanced Enzyme Production. In : Biotechnology and Biology of Trichoderma: Elsevier, pp. 193–200.

Ghose, T. K.; Sahai, Vikram (1979): Production of cellulases by *Trichoderma reesei* QM 9414 in fed-batch and continuous-flow culture with cell recycle. Biotechnol. Bioeng. 21 (2), pp. 283–296. DOI: 10.1002/bit.260210213.

Global Agriculture Information Network (2015): EU Biofuels Annual 2015 (NL5028).

Gonçalves Roque, Tamiris (2019): Application de la méthodologie Scale-down à l'étude de l'effet du mélange. Master Thesis. IFPEN.

Hardy, Nicolas (2016): Identification des critères d'extrapolation du procédé de production de cellulases par *Trichoderma reesei* en utilisant l'approche " scale-down ". PhD. IFPEN.

Harman, Gary E.; Kubicek, C. P. (1998): Trichoderma And Gliocladium, Volume 2: CRC Press.

Harris, Steven D. (2008): Branching of fungal hyphae. Regulation, mechanisms and comparison with other branching systems. Mycologia 100 (6), pp. 823–832. DOI: 10.3852/08-177.

Hayakawa, Yugo; Ishikawa, Eri; Shoji, Jun-Ya; Nakano, Hiroyuki; Kitamoto, Katsuhiko (2011): Septum-directed secretion in the filamentous fungus Aspergillus oryzae. Molecular microbiology 81 (1), pp. 40–55. DOI: 10.1111/j.1365-2958.2011.07700.x.

Hemansi; Chakraborty, Subhojit; Yadav, Garima; Saini, Jitendra Kumar; Kuhad, Ramesh Chander (2019): Comparative Study of Cellulase Production Using Submerged and Solid-State Fermentation. In : New and Future Developments in Microbial Biotechnology and Bioengineering: Elsevier, pp. 99–113.

Hendy, Neil A.; Wilke, Charles R.; Blanch, Harvey W. (1984): Enhanced cellulase production in fed-batch culture of *Trichoderma reesei* C30. Enzyme and Microbial Technology 6 (2), pp. 73–77. DOI: 10.1016/0141-0229(84)90038-3.

Herve, Guyomard; Agneta, Forslund; Yves, Dronne (2011): Biofuels and World Agricultural Markets. Outlook for 2020 and 2050. Marco Aurelio Dos Santos Bernardes (Ed.): Does Money Grow on Trees? People's Willingness to Pay for Cellulosic Wood Ethanol: INTECH Open Access Publisher.

Hossain, Md Shahadat; Theodoropoulos, Constantinos; Yousuf, Abu (2019): Techno-economic evaluation of heat integrated second generation bioethanol and furfural coproduction. Biochemical Engineering Journal 144, pp. 89–103. DOI: 10.1016/j.bej.2019.01.017.

Jacobsen, Sigrid E.; Wyman, Charles E. (2000): Cellulose and Hemicellulose Hydrolysis Models for Application to Current and Novel Pretreatment Processes. ABAB 84-86 (1-9), pp. 81–96. DOI: 10.1385/ABAB:84-86:1-9:81.

Jarvis, Mike (2003): Cellulose stacks up. Nature 426 (6967), pp. 611–612. DOI: 10.1038/426611a.

Jayasekara, Sandhya; Ratnayake, Renuka (2019): Microbial Cellulases. An Overview and Applications. Alejandro Rodríguez Pascual, Maria E. Eugenio Martin (Eds.): Cellulose. London: IntechOpen.

Jourdier, Etienne (2012): Modélisation et optimisation de la production de cellulases par Modélisation et optimisation de la production de cellulases par*Trichoderma reesei* pour les bioraffineries lignocellulosiques. PhD. IFPEN.

Keshavarz, Behnam; Khalesi, Mohammadreza (2016): *Trichoderma reesei*, a superior cellulase source for industrial applications. Biofuels 7 (6), pp. 713–721. DOI: 10.1080/17597269.2016.119 2444.

Kunamneni, Adinarayana; Plou, Francisco J.; Alcalde, Miguel; Ballesteros, Antonio (2014): Trichoderma Enzymes for Food Industries. : Biotechnology and Biology of Trichoderma: Elsevier, pp. 339–344.

KÜÜT, A.; RITSLAID, K.; OLT, J. (2011): Study of potential uses for farmstead ethanol as motor fuel. Agronomy research (Tartu) 9, 125-134.

L. Rocha-Meneses; Merlin Raud; Kaja Orupõld; Timo Kikas (2017): Second-generation bioethanol production. A review of strategies for waste valorisation. Agronomy Research 15 (3), pp. 830–847.

Laursen W. (2006): Students take a green initiative. Chemical Engineer -London then Rugby 774, pp. 32–34.

Lo, Chi-Ming; Zhang, Qin; Callow, Nicholas V.; Ju, Lu-Kwang (2010): Roles of extracellular lactose hydrolysis in cellulase production by *Trichoderma reesei* Rut C30 using lactose as inducing substrate. Process Biochemistry 45 (9), pp. 1494–1503. DOI: 10.1016/j.procbio.2010.05.031.

Ma, Lijuan; Li, Chen; Yang, Zhenhua; Jia, Wendi; Zhang, Dongyuan; Chen, Shulin (2013): Kinetic studies on batch cultivation of *Trichoderma reesei* and application to enhance cellulase production by fed-batch fermentation. Journal of Biotechnology 166 (4), pp. 192–197. DOI: 10.1016/j.jbiotec.2013.04.023.

Marten, M. R.; Velkovska, S.; Khan, S. A.; Ollis, D. F. (1996): Rheological, Mass Transfer, and Mixing Characterization of Cellulase-Producing *Trichoderma reesei* Suspensions. Biotechnol. Prog. 12 (5), pp. 602–611. DOI: 10.1021/bp950066b.

McKendry, Peter (2002): Energy production from biomass (part 1). Overview of biomass. Bioresource Technology 83 (1), pp. 37–46. DOI: 10.1016/S0960-8524(01)00118-3.

Mojsov, K. D. (2016): Aspergillus Enzymes for Food Industries. In : New and Future Developments in Microbial Biotechnology and Bioengineering: Elsevier, pp. 215–222.

Muthuvelayudham, R.; Viruthagiri, T. (2006): Optimization and modeling of cellulase protein from *Trichoderma reesei* Rut C30 using mixed substrate.

Naik, S. N.; Goud, Vaibhav V.; Rout, Prasant K.; Dalai, Ajay K. (2010): Production of first and second generation biofuels. A comprehensive review. Renewable and Sustainable Energy Reviews 14 (2), pp. 578–597. DOI: 10.1016/j.rser.2009.10.003.

Nevalainen, Helena; Peterson, Robyn (2014): Making recombinant proteins in filamentous fungi- are we expecting too much? Frontiers in microbiology 5, p. 75. DOI: 10.3389/fmicb.2014.00075.

Nguyen, Duc; Nitayavardhana, Saoharit; Sawatdeenarunat, Chayanon; Surendra, K. C.; Khanal, Samir Kumar (2019): Biogas Production by Anaerobic Digestion. Status and Perspectives. Ashok Pandey, Christian Larroche, Edgard Gnansounou, Samir Kumar Khanal, Claude-Gilles Dussap, Steven Ricke (Eds.): Biofuels. Alternative Feedstocks and Conversion Processes for the Production of Liquid and Gaseous Biofuels / edited by Ashok Pandey, Christian Larroche, Claude-Gilles Dussap, Edgard Gnansounou, Samir Kumar Khanal, and Steve Ricke. Second edition. San Diego, CA: Academic Press (Biomass, Biofuels, Biochemicals), pp. 763–778.

Nielsen, Jens; Villadsen, John (1992): Modelling of microbial kinetics. Chemical Engineering Science 47 (17-18), pp. 4225–4270. DOI: 10.1016/0009-2509(92)85104-J.

Nigam, Poonam Singh; Singh, Anoop (2011): Production of liquid biofuels from renewable resources. Progress in Energy and Combustion Science 37 (1), pp. 52–68. DOI: 10.1016/j.pecs.2010.01.003.

Patel, Jignesh P.; Parsania, Parsotam H. (2018): Characterization, testing, and reinforcing materials of biodegradable composites. In : Biodegradable and Biocompatible Polymer Composites: Elsevier, pp. 55–79.

Pejin, D.; Mojović, L. J.; Vučurović, V.; Pejin, J.; Denčić, S.; Rakin, M. (2009): Fermentation of wheat and triticale hydrolysates. A comparative study. Fuel 88 (9), pp. 1625–1628. DOI: 10.1016/j.fuel.2009.01.011.

Percival Zhang, Y-H; Himmel, Michael E.; Mielenz, Jonathan R. (2006): Outlook for cellulase improvement. Screening and selection strategies. Biotechnology Advances 24 (5), pp. 452–481. DOI: 10.1016/j.biotechadv.2006.03.003.

Portnoy, Thomas; Margeot, Antoine; Linke, Rita; Atanasova, Lea; Fekete, Erzsébet; Sándor, Erzsébet et al. (2011): The CRE1 carbon catabolite repressor of the fungus *Trichoderma reesei*. A master regulator of carbon assimilation. BMC genomics 12, p. 269. DOI: 10.1186/1471-2164-12-269.

Prado Barragán, L. A.; Figueroa, J.J.B.; Rodríguez Durán, L. V.; Aguilar González, C. N.; Hennigs, C. (2016): Fermentative Production Methods. Palmiro Poltronieri, Oscar Fernando D'Urso (Eds.): Biotransformation of agricultural waste and by-products. The food, feed, fibre, fuel (4F) economy / edited by Palmiro Poltronieri, Oscar Fernando D'Urso. Amsterdam: Elsevier, pp. 189–217.

Rakshit, S. K.; Sahai, V. (1991): Optimal control strategy for the enhanced production of cellulase enzyme using the new mutant *Trichoderma reesei* E-12. Bioprocess Engineering 6 (3), pp. 101–107. DOI: 10.1007/BF00369062.

Raud, M.; Rain Kesperi; Tõnu Oja; Jüri Olt; Timo Kikas (2014): Utilization of urban waste in bioethanol production. Potential and technical solutions. Agronomy Research 12 (2), pp. 397–406.

Robak, Katarzyna; Balcerek, Maria (2018): Review of Second-Generation Bioethanol Production from Residual Biomass. Food Technol. Biotechnol. 56 (2). DOI: 10.17113/ftb.56.02.18.5428.

Saloheimo, Markku; Pakula, Tiina M. (2012): The cargo and the transport system. Secreted proteins and protein secretion in *Trichoderma reesei* (Hypocrea jecorina). Microbiology (Reading, England) 158

(Pt 1), pp. 46–57. DOI: 10.1099/mic.0.053132-0.

Schmoll, Monika; Dattenböck, Christoph (2016): Gene Expression Systems in Fungi. Advancements and Applications. Cham: Springer International Publishing.

Seidl, V.; Seibel, C.; Kubicek, C. P.; Schmoll, M. (2009): Sexual development in the industrial workhorse *Trichoderma reesei*. Proceedings of the National Academy of Sciences 106 (33), pp. 13909–13914. DOI: 10.1073/pnas.0904936106.

Shelley Minteer (2016): Alcoholic Fuels: CRC Press.

Sigoillot, Jean-Claude; Faulds, Craig (2011): Second Generation Bioethanol. Carlos Ricardo Soccol, Satinder Kaur Brar, Craig Faulds, Luiz Pereira Ramos (Eds.): Green Fuels Technology. Biofuels: Springer, pp. 213–239.

Simo Ellilä; Lucas Fonseca; Cristiane Uchima; Junio Cota; Gustavo Henrique Goldman; Markku Saloheimo et al. (2017): Development of a low-cost cellulase production process using *Trichoderma reesei* for Brazilian biorefineries. Biotechnol Biofuels 10 (1), pp. 1–17. DOI: 10.1186/s13068-017-0717-0.

Soni, Sanjeev Kumar; Sharma, Amita; Soni, Raman (2018): Cellulases. Role in Lignocellulosic Biomass Utilization. Methods in molecular biology (Clifton, N.J.) 1796, pp. 3–23. DOI: 10.1007/978-1-4939-7877-9_1.

Sun, Ye; Cheng, Jiayang (2002): Hydrolysis of lignocellulosic materials for ethanol production. A review. Bioresource Technology 83 (1), pp. 1–11. DOI: 10.1016/S0960-8524(01)00212-7.

Tholudur, Arun; Ramirez, W. Fred; McMillan, James D. (1999): Mathematical modeling and optimization of cellulase protein production using*Trichoderma reesei* RL-P37. Biotechnol. Bioeng. 66 (1), pp. 1–16. DOI: 10.1002/(SICI)1097-0290(1999)66:1¡1::AID-BIT1¿3.0.CO;2-K.

Thomas, Leya; Larroche, Christian; Pandey, Ashok (2013): Current developments in solid-state fermentation. Biochemical Engineering Journal 81, pp. 146–161. DOI: 10.1016/j.bej.2013.10.013.

Tye, Ying Ying; Lee, Keat Teong; Wan Abdullah, Wan Nadiah; Leh, Cheu Peng (2016): The world availability of non-wood lignocellulosic biomass for the production of cellulosic ethanol and potential pretreatments for the enhancement of enzymatic saccharification. Renewable and Sustainable Energy Reviews 60, pp. 155–172. DOI: 10.1016/j.rser.2016.01.072.

Valkonen, Mari; Kalkman, Eric R.; Saloheimo, Markku; Penttilä, Merja; Read, Nick D.; Duncan, Rory R. (2007): Spatially segregated SNARE protein interactions in living fungal cells. The Journal of biological chemistry 282 (31), pp. 22775–22785. DOI: 10.1074/jbc.M700916200.

Velkovska, Svetlana; Marten, Mark R.; Ollis, David F. (1997): Kinetic model for batch cellulase production by *Trichoderma reesei* RUT C30. Journal of Biotechnology 54 (2), pp. 83–94. DOI: 10.1016/S0168-1656(97)01669-6.

Zabed, H.; Sahu, J. N.; Boyce, A. N.; Faruq, G. (2016): Fuel ethanol production from lignocellulosic biomass. An overview on feedstocks and technological approaches. Renewable and Sustainable Energy Reviews 66, pp. 751–774. DOI: 10.1016/j.rser.2016.08.038.

Zhang, Jiajia; Chen, Yumeng; Wu, Chuan; Liu, Pei; Wang, Wei; Wei, Dongzhi (2019): The transcription factor ACE3 controls cellulase activities and lactose metabolism via two additional regulators in the fungus *Trichoderma reesei*. The Journal of biological chemistry 294 (48), pp. 18435–18450. DOI: 10.1074/jbc.RA119.008497.

Appendix A

Full set of equations for the 2 reactor system

Reactor 1 calculations (aerobic reactor)

Kinetic Calculations

$$\mu\_r1 = \frac{\mu_{\text{max}} \times [S]\_r1}{K_{\text{S}\mu} + [S]\_r1} \times \frac{[O_2]\_r1}{K_{\text{O}_2\mu} + [O_2]\_r1} \tag{A.1}$$

$$q_{\text{p}}\_r1 = (\frac{q_{\text{pmax}} - q_{\text{pmin}}}{1 + \frac{[X]\_r1}{K_{\text{iXP}}}} + q_{\text{pmin}}) \times \frac{[S]\_r1}{K_{\text{SP}} + [S]\_r1} \times \frac{[O_2]\_r1}{K_{\text{O}_2\text{P}} + [O_2]\_r1} \times \frac{K_{\text{iSP}}}{K_{\text{iSP}} + [S]\_r1} \tag{A.2}$$

$$m_{\text{s}}\_r1 = m_{\text{s max}} \frac{[S]\_r1}{K_{\text{s M}} + [S]\_r1} \times \frac{[O_2]\_r1}{K_{\text{O}_2\text{ M}} + [O_2]\_r1} \tag{A.3}$$

$$q_{\text{s}}\_r1 = \frac{\mu\_r1}{Y_{\text{x/s}}} + \frac{q_{\text{p}}\_r1}{Y_{\text{p/s}}} + m_{\text{s}}\_r1 \tag{A.4}$$

$$q_{\text{O}_2\text{-r1}} = \frac{\mu\_r1}{Y_{\text{x/O}_2}} + \frac{q_{\text{p}}\_r1}{Y_{\text{p/O}_2}} + Y_{\text{O}_2/\text{s}}{}^{\text{m}} \times m_{\text{s}}\_r1 \tag{A.5}$$

Gas phase calculations

$$\frac{d[O_2]_{\text{gas}}\_r1}{dt} = \frac{(Q_{\text{O}_2\text{ in}}\_r1 - Q_{\text{O}_2\text{ out}}\_r1 - OTR\_r1 \times V_{\text{L}}\_r1)}{V_{\text{ga}}\_r1} + \frac{(Qrg_{\text{2-1}} \times f_{\text{O}_2}\_r2 - Qrg_{\text{1-2}} \times f_{\text{O}_2}\_r1) \times 32}{V_{\text{gas}}\_r1} \tag{A.6}$$

$$f_{\text{O}_2}\_r1 = \frac{[O_2]_{\text{gas}}\_r1}{32} \times \frac{RT}{P} \times 1000 \tag{A.7}$$

$$OTR\_r1 = k_{\text{l}}a\_r1(K_{\text{H}} \times f_{\text{O}_2}\_r1 \times P \times 32 - [O_2]\_r1) \tag{A.8}$$

$$Q_{\text{N}_2\text{ out}}\_r1 = Q_{\text{N}_2\text{ in}}\_r1 + (Qrg_{\text{2-1}} \times (1 - f_{\text{O}_2}\_r2) - Qrg_{\text{1-2}} \times (1 - f_{\text{O}_2}\_r1)) \times 28 \tag{A.9}$$

$$Q_{\text{O}_2\text{ out}}\_r1 = \frac{Q_{\text{N}_2\text{ out}}\_r1}{28} \frac{1 - f_{\text{O}_2}\_r1}{f_{\text{O}_2}\_r1} \times 32 \tag{A.10}$$

Liquid phase calculations

$$\frac{d[X]\_r1}{dt} = \mu[X] - \frac{[X]\_r1}{V_{\mathrm{L}}\_r1}\Delta Q_{\mathrm{v}}\_r1 + \frac{Q_{\mathrm{r\ 2\text{-}1}}[X]\_r2 - Q_{\mathrm{r\ 1\text{-}2}}[X]\_r1}{V_{\mathrm{L}}\_r1} \tag{A.11}$$

$$\frac{d[P]\_r1}{dt} = q_{\mathrm{p}}\_r1[P]\_r1 - \frac{[P]\_r1}{V_{\mathrm{L}}\_r1}\Delta Q_{\mathrm{v}}\_r1 + \frac{Q_{\mathrm{r\ 2\text{-}1}}[P]\_r2 - Q_{\mathrm{r\ 1\text{-}2}}[P]\_r1}{V_{\mathrm{L}}\_r1} \tag{A.12}$$

$$\frac{d[S]\_r1}{dt} = -q_{\mathrm{s}}\_r1[X]\_r1 + \frac{Q_{\mathrm{fb}}[S_{\mathrm{fb}}] - [S]\_r1\Delta Q_{\mathrm{v}}\_r1}{V_{\mathrm{L}}\_r1} + \frac{Q_{\mathrm{r\ 2\text{-}1}}[S]\_r2 - Q_{\mathrm{r\ 1\text{-}2}}[S]\_r1}{V_{\mathrm{L}}\_r1} \tag{A.13}$$

$$\frac{d[O_2]\_r1}{dt} = -q_{\mathrm{O_2\_r1}}[O_2]\_r1 + k_{\mathrm{L}}a\_r1([O_2]^{*}\_r1 - [O_2]\_r1) - \frac{[O_2]\_r1}{V_{\mathrm{L}}\_r1}\Delta Q_{\mathrm{v}}\_r1 + \frac{Q_{\mathrm{r\ 2\text{-}1}}[O_2]\_r2 - Q_{\mathrm{r\ 1\text{-}2}}[O_2]\_r1}{V_{\mathrm{L}}\_r1} \tag{A.14}$$

$$\Delta Q_{\mathrm{v}}\_r1 = \frac{V_{\mathrm{L}}\_r1}{dt} = Q_{\mathrm{base}} + Q_{\mathrm{fb}} - Q_{\mathrm{evp}}\_r1 \tag{A.15}$$

Reactor 2 calculations (anaeroobic reactor)

Kinetic Calculations

$$\mu\_r2 = \frac{\mu_{\mathrm{max}} \times [S]\_r2}{K_{\mathrm{S\mu}} + [S]\_r2} \times \frac{[O_2]\_r2}{K_{\mathrm{O_{2\mu}}} + [O_2]\_r2} \tag{A.16}$$

$$q_{\mathrm{p}}\_r2 = (\frac{q_{\mathrm{pmax}} - q_{\mathrm{pmin}}}{1 + \frac{[X]\_r2}{K_{\mathrm{iXP}}}} + q_{\mathrm{pmin}}) \times \frac{[S]\_r2}{K_{\mathrm{SP}} + [S]\_r2} \times \frac{[O_2]\_r2}{K_{\mathrm{O_2P}} + [O_2]\_r2} \times \frac{K_{\mathrm{iSP}}}{K_{\mathrm{iSP}} + [S]\_r2} \tag{A.17}$$

$$m_{\mathrm{s}}\_r2 = m_{\mathrm{s\ max}}\frac{[S]\_r2}{K_{\mathrm{s\ M}} + [S]\_r2} \times \frac{[O_2]\_r2}{K_{\mathrm{O_2\ M}} + [O_2]\_r2} \tag{A.18}$$

$$q_{\mathrm{s}}\_r2 = \frac{\mu\_r2}{Y_{\mathrm{x/s}}} + \frac{q_{\mathrm{p}}\_r2}{Y_{\mathrm{p/s}}} + m_{\mathrm{s}}\_r2 \tag{A.19}$$

$$q_{\mathrm{O_2\_r2}} = \frac{\mu\_r2}{Y_{\mathrm{x/O_2}}} + \frac{q_{\mathrm{p}}\_r2}{Y_{\mathrm{p/O_2}}} + Y_{\mathrm{O_2/s}}{}^{\mathrm{m}} \times m_{\mathrm{s}}\_r2 \tag{A.20}$$

Gas phase calculations

$$\frac{d[O_2]_{\mathrm{gas}}\_r2}{dt} = \frac{(Q_{\mathrm{O_2\ in}}\_r2 - Q_{\mathrm{O_2\ out}}\_r2 - OTR\_r2 \times V_{\mathrm{L}}\_r2)}{V_{\mathrm{ga}}\_r2} + \frac{(Qrg_{\mathrm{1\text{-}2}} \times f_{\mathrm{O_2}}\_r1 - Qrg_{\mathrm{2\text{-}1}} \times f_{\mathrm{O_2}}\_r2) \times 32}{V_{\mathrm{gas}}\_r2} \tag{A.21}$$

$$f_{\mathrm{O_2}}\_r2 = \frac{[O_2\_r2]_{\mathrm{gas}}\_r2}{32} \times \frac{RT}{P} \times 1000 \tag{A.22}$$

$$OTR\_r2 = k_{\mathrm{l}}a\_r2(K_{\mathrm{H}} \times f_{\mathrm{O_2}}\_r2 \times P \times 32 - [O_2]\_r2) \tag{A.23}$$

$$Q_{\mathrm{N_2\ out}}\_r2 = Q_{\mathrm{N_2\_r2\ in}}\_r2 + (Qrg_{\mathrm{1\text{-}2}} \times (1 - f_{\mathrm{O_2}}\_r1) - Qrg_{\mathrm{2\text{-}1}} \times (1 - f_{\mathrm{O_2}}\_r2)) \times 28 \tag{A.24}$$

$$Q_{\mathrm{O_2\ out}}\_r2 = \frac{Q_{\mathrm{N_2\ out}}\_r2}{28}\frac{1 - f_{\mathrm{O_2}}\_r2}{f_{\mathrm{O_2}}\_r2} \times 32 \tag{A.25}$$

Liquid phase calculations

$$\frac{d[X]\_r2}{dt} = \mu[X] - \frac{[X]\_r2}{V_{\mathsf{L}}\_r2}\Delta Q_{\mathsf{v}}\_r2 + \frac{Q_{\mathsf{r\ 1\text{-}2}}[X]\_r1 - Q_{\mathsf{r\ 2\text{-}1}}[X]\_r2}{V_{\mathsf{L}}\_r2} \tag{A.26}$$

$$\frac{d[P]\_r2}{dt} = q_{\mathsf{p}}\_r2[P]\_r2 - \frac{[P]\_r2}{V_{\mathsf{L}}\_r2}\Delta Q_{\mathsf{v}}\_r2 + \frac{Q_{\mathsf{r\ 1\text{-}2}}[P]\_r1 - Q_{\mathsf{r\ 2\text{-}1}}[P]\_r2}{V_{\mathsf{L}}\_r2} \tag{A.27}$$

$$\frac{d[S]\_r2}{dt} = -q_{\mathsf{s}}\_r2[X]\_r2 - \frac{[S]\_r2\Delta Q_{\mathsf{v}}\_r2}{V_{\mathsf{L}}\_r2} + \frac{Q_{\mathsf{r\ 1\text{-}2}}[S]\_r1 - Q_{\mathsf{r\ 2\text{-}1}}[S]\_r2}{V_{\mathsf{L}}\_r2} \tag{A.28}$$

$$\frac{d[O_2]\_r2}{dt} = -q_{\mathsf{O_2}\_\mathsf{r2}}[O_2]\_r2 + k_{\mathsf{L}}a\_r2([O_2]^{*}\_r2 - [O_2]\_r2) - \frac{[O_2]\_r2}{V_{\mathsf{L}}\_r2}\Delta Q_{\mathsf{v}}\_r2 + \frac{Q_{\mathsf{r\ 1\text{-}2}}[O_2]\_r1 - Q_{\mathsf{r\ 2\text{-}1}}[O_2]\_r2}{V_{\mathsf{L}}\_r2} \tag{A.29}$$

$$\Delta Q_{\mathsf{v}}\_r2 = \frac{V_{\mathsf{L}}\_r2}{dt} = -Q_{\mathsf{evp}}\_r2 \tag{A.30}$$

Appendix B

Modeling results of the experiment repetitions of K1439

Figure B.1: Modelling results for the culture K1526, in which the marker ◆ represents the experimental points of biomass concentration and the ■ represents the experimental points of protein concentration. The — represents the model prediction for the biomass concentration, the — represents the model prediction for the protein concentration and the — represents the model predictions for the substrate concentration.

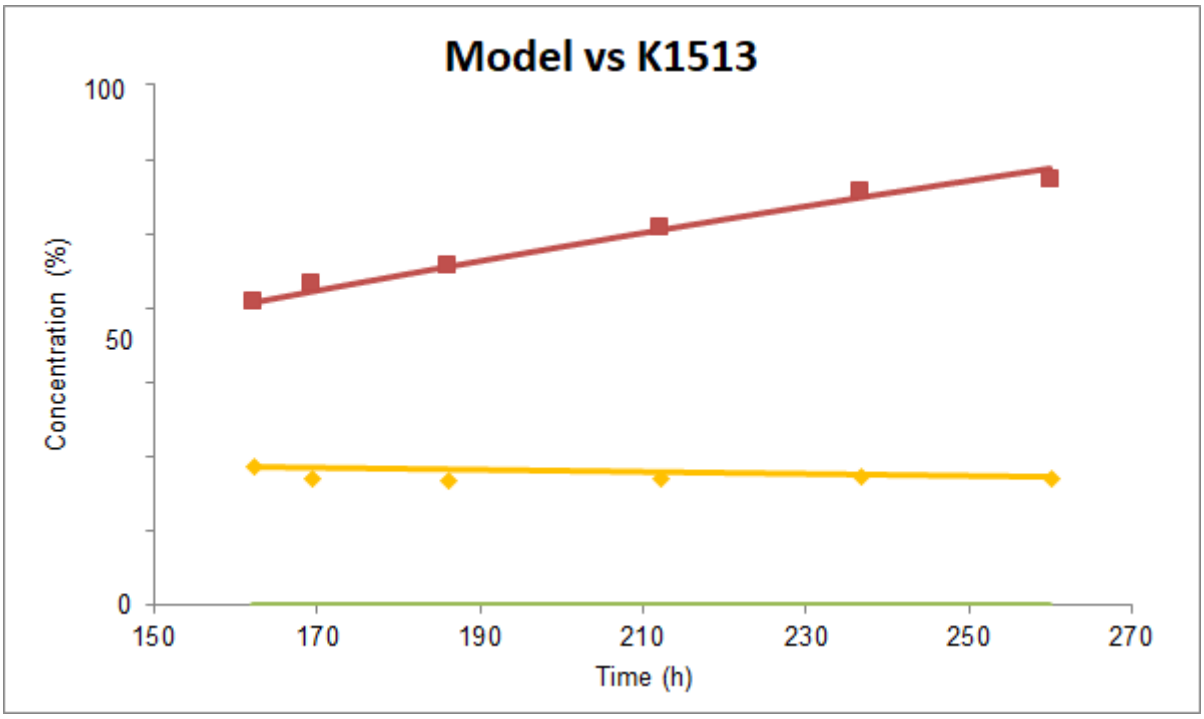

Figure B.2: Modelling results for the culture K1513, in which the marker ◆ represents the experimental points of biomass concentration and the ■ represents the experimental points of protein concentration. The — represents the model prediction for the biomass concentration, the — represents the model prediction for the protein concentration and the — represents the model predictions for the substrate concentration.

Table B.1: Comparison between the q_p values from the experimental experiments and modelling results.

Experiment	**q_p^* experimental (%)**	**q_p^* model (%)**
K1526	58	62
K1513	61	60